Materials for Optimized P&A Performance

Potential Utilization of Geopolymers

by
Mahmoud Khalifeh

Thesis submitted in partial fulfillment of
the requirements for the degree of
DOCTOR OF PHILOSOPHY
(PhD)

Faculty of Science and Technology
Department of Petroleum Engineering

2016

University of Stavanger
N-4036 Stavanger
NORWAY
www.uis.no

ISBN: 978-82-7644-647-0
ISSN: 1890-1387

PhD thesis UiS no. 292

PREFACE

This thesis is submitted in partial fulfillment of the requirements for the degree of PhD (Doctor of Philosophy) in Petroleum Engineering at the University of Stavanger (UiS), Norway. The PhD program was financially funded by DrillWell - Drilling and Well Centre for Improved Recovery, a research cooperation between IRIS, NTNU, SINTEF, and UiS. The thesis presents results of the research work conducted at the Department of Petroleum Engineering, UiS from September 2012 to May 2016. The outcome of this study is given through six published papers, two peer-reviewed scientific journal articles and four presented conference papers. In addition, two more articles have been submitted to peer-reviewed scientific journals. All the papers are attached at the end of this thesis. The papers are enumerated in a chronological order using Roman numerals. The Roman numerals have also been used when referring to these papers in the present review.

In Paper I, techniques and materials, which are used in Plug and Abandonment (P&A) operations in the North Sea, are presented. This paper includes an overview of potential well barrier materials with their concerns and advantages. Furthermore, some case histories of performed P&A operations were reviewed.

Paper II discusses usability of geopolymers in P&A operations. Besides rheological behavior of geopolymers, such as viscosity and pumpability, bulk shrinkage, compressive strength development, and microstructure of fly ash-based geopolymers are considered.

Paper III presents the influence of alkali concentration and curing temperature on the chemo-physical and rheology of fly ash-based geopolymers. The paper brings a consecutive reaction forward, which was activated at an elevated temperature of 125℃ and high concentration of alkali solution. The phenomenon significantly reduces the compressive strength of the geopolymers.

Paper IV introduces a new rock-based geopolymer. The paper presents the synthesis and characterization of an aplite rock-based geopolymer. The geopolymers were characterized both in macro- and micro-levels.

Paper V presents possible utilization of the geopolymers, synthesized during work presented in paper IV, for permanent zonal isolation and well plugging. Paper V considers the placeability of the aplite rock-based geopolymers by

changing of mix ratios. Moreover, effects of each mix change on rheological and mechanical properties of the geopolymers were studied.

Paper VI presents the influence of a retarder on the pumpability and setting time of the aplite rock-based geopolymers. Sucrose was used as a retarder and it was important to investigate the effect of sucrose on rheology and physical properties of the geopolymers. Young's modulus, Poisson's ratio, bulk modulus, and compressive strength of the geopolymers were studied, in addition to axial and radial creep.

Paper VII introduces synthesis of a new geopolymer produced from a mine waste. The paper presents the influence of particle size, Ground Granulated Blast Furnace Slag (GGBFS), and alkali solution on norite-based geopolymers. The compressive strength and microstructure of the geopolymers were studied by performing compression tests and XRD, respectively.

Paper VIII presents the long-term integrity of aplite rock-based geopolymers, which were exposed to hydrogen sulfide, crude oil, and brine for different time intervals.

To my family; especially my kind brother,
for all the support and motivation

ACKNOWLEDGEMENTS

The work presented in this dissertation has for the major part been carried out at the University of Stavanger, at the Department of Petroleum Engineering. The Department of Petroleum Engineering has provided me with excellent working conditions and I would like to thank all my colleagues for their support.

I would like to give special thanks to my supervisors, Prof. H. Hodne, Prof. A. Saasen, and Dr. T. Vrålstad for their patience and support through the present work.

I gratefully acknowledge the Research Council of Norway, ConocoPhillips, Det norske oljeselskap, Statoil, Wintershall, and Lundin Norway AS for financing the work through the research centre DrillWell - Drilling and Well Centre for Improved Recovery, a research cooperation between IRIS, NTNU, SINTEF, and UiS.

A special thanks to European Synchrotron Radiation Facility (ESRF) for provision of synchrotron beam time and technical assistance from the SNBL-consortium.

Lastly, I would also like to thank my family for their love and encouragement. Without them, I would never have finalized my Ph.D. work. Thank you.

Mahmoud Khalifeh

Stavanger, Norway

May 2016

LIST OF PUBLICATIONS

I. Khalifeh, M., Hodne, H., Saasen, A., and Vrålstad, T. 2013. *Techniques and materials for North Sea plug and abandonment operations*. Paper OTC-23915 presented at the Offshore Technology Conference, 6-9 May, Houston, Texas, USA.

II. Khalifeh, M., Saasen, A., Vrålstad, T., and Hodne, H. 2014. *Potential utilization of geopolymers in plug and abandonment operations*. Paper SPE-169231 presented at the SPE Bergen One Day Seminar held in Grieghallen, Bergen, Norway, 2 April 2014.

III. Khalifeh, M., Saasen, A., Vrålstad, T., and Hodne, H. 2014. *Potential utilization of class C fly ash-based geopolymer in oil well cementing operations*. Journal of Cement and Concrete Composites 53 (2014) 10-17.

IV. Khalifeh, M., Saasen A., Vrålstad, T., Larsen, H.B., and Hodne, H. 2015. *Experimental study on the synthesis and characterization of aplite rock-based geopolymers*. Journal of Sustainable Cement-Based Materials.

V. Khalifeh, M., Saasen, A., Vrålstad, T., Larsen, H.B., Hodne, H. 2015. *Cap rock restoration in plug and abandonment operations; possible utilization of aplite-based geopolymers for permanent zonal isolation and well plugging*. Paper SPE-17547-MS presented at the SPE Offshore Europe and Conference and Exhibition held in Aberdeen, Scotland, UK, 8-11 September 2015.

VI. Khalifeh, M., Saasen, A., Korsnes, R.I., and Hodne, H. 2015. *Cap rock restoration in plug and abandonment operations; possible utilization of rock-based geopolymers for permanent zonal isolation and well plugging*. Paper IPTC-18454-MS presented at the International Petroleum Technology Conference held in Doha, Qatar, 7-9 December 2015.

VII. Khalifeh, M., Saasen, A., Larsen, H.B., and Hodne, H. Submitted. *Experimental study on the formation (development) and characterization of norite-based geopolymer produced from an ilmenite mine waste stream, polymerized with NaOH and KOH solutions*. Submitted to a scientific journal in June 2015.

VIII. Khalifeh, M., Todorovic, J., Vrålstad, T., Saasen, A., and Hodne, H. Submitted. *Long-term durability of rock-based geopolymers aged at downhole conditions for oil well cementing operations*. Submitted to a scientific journal in February 2016.

TABLE OF CONTENTS

LIST OF FIGURES

LIST OF TABLES

NOMENCLATURE

Latin

ΔL	Changes in length
Δr	Changes in radius
A	Specimen surface area
Å	Angstrom
Bc	Bearden units of consistency
D	Specimen diameter
d	Distance between two adjacent planes of atoms
dp	Applied pressure changes
dV	Volume changes
E	Young's modulus
F	Maximum applied force
H	Length of specimen
K	Potassium
m	Mass of core holder
N	Newton
N/A	Not available
pqr	Additional distance
t	Time
T	Torque
V	Specimen volume

Greek

κ	Bulk modulus
θ	Angle of incidence
λ	Wavelength of X-rays
μ	Micron
ν	Poisson's ratio
ρ	Water density
σ	Compressive strength
σ_x	Tensile strength

Abbreviations

3D	Three dimensional
Al	Aluminum
BHCT	Bottom Hole Circulating Temperature
BSE	Backscattered Electron
℃	Degree Celsius
Ca	Calcium
C-A-S-H	Calcium Alumino-Silicate Hydrate

cc	Cubic centimeter
CFA	Class C Fly Ash
CO_2	Carbon dioxide
DEA	Danish Energy Agency
EDX	Energy-Dispersive X-ray Spectroscopy
Fe	Iron
g	grams
GGBFS	Ground Granulated Blast Furnace Slag
HPHT	High Pressure – High Temperature
HSE	Health, Safety, and Environment
K^+	Potassium ion
K_2SiO_3	Potassium silicate solution
Mg	Magnesium
MPE	Ministry of Petroleum and Energy
MPro	Mechanical Properties Analyzer
Na^+	Sodium ion
Na_2O	Sodium oxide
Na_2SiO_3	Sodium silicate solution
N-A-S-H	Sodium Aluminosilicate Hydrate
NCS	Norwegian Continental Shelf
NPD	Norwegian Petroleum Directorate
O	Oxygen
OH^-	Hydroxide
P&A	Plug and Abandonment
PSA	Petroleum Safety Authority
RPM	Rotations per minutes
S^{-2}	Sulfide
SEM	Scanning Electron Microscopy
SF	Shrinkage Factor
Si	Silicon
SiO_2	Silicon dioxide
Ti	Titanium
UCA	Ultrasonic Cement Analyzer
UCS	Uniaxial Compressive Strength
UKOOA	United Kingdom Offshore Operators Association

Chapter 1

Introduction

When a well reaches the end of its life-cycle, it must be permanently plugged and abandoned. Plug and abandonment (P&A) can easily contribute with 25% of the total drilling costs of exploration wells offshore Norway. The costs of running a P&A operation on some offshore production wells may have a cost impact similar to the cost of the original drilling operation. Generally, the purpose of P&A is to restore the cap-rock functionality to preserve well-integrity permanently. In order to succeed, appropriate permanent barriers shall be placed across suitable formations by utilizing relevant equipment. Therefore, the downhole P&A activities could be categorized into two general categories: surface and subsurface activities. Subsurface activities can be divided into two sectors: tools and techniques and plugging materials. Since the scope of this work considers usability of particular plugging materials (geopolymers) the P&A scope will be reviewed in the following section briefly.

1.1. Plug and Abandonment

P&A is a collection of operations taken to isolate and protect the environment and all fresh water zones and surroundings from a source of potential flow. The potential source is a formation with permeability and it may be a water- or a hydrocarbon-bearing zone. The fundamental of P&A operations varies, whether the well is offshore or onshore or if the well is going to be abandoned permanently or temporarily (*NORSOK D-010 2013; Oil & Gas UK 2012a*).

1.2. Past, Present, and Future of Plugged and Abandoned Wells in Norway

Since the first discovery on the Norwegian Continental Shelf (NCS) in 1966 until June 2015, nearly 5579 wells have been drilled. Of these wells, 4037 are development wells and 1542 are exploration wells. Of the exploration wells, 1480 have been permanently plugged and abandoned. Of the development wells, 1400 have been permanently abandoned and 467 are in temporary abandonment status (*Norwegian Petroleum Directorate 2015*). It is estimated that 2637 development wells need to be plugged and abandoned in the near future, **Fig. 1.1a-b**. In addition, the number of wells which will be drilled in the future, should be added for plug and abandonment.

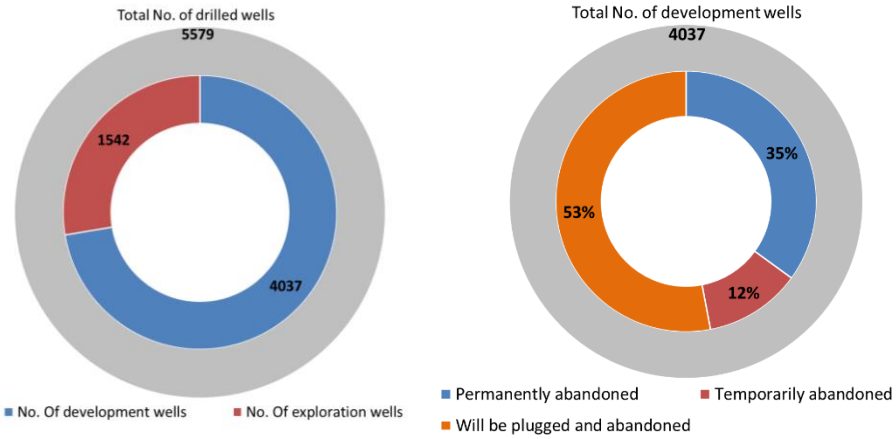

a) Total number of all drilled wells.

b) Total number of all drilled development wells.

Figure 1.1 A status overview of all drilled wells on the Norwegian sector of the NCS.

1.3. Abandonment Types

For both onshore and offshore wells, the decision to plug and abandon a well is invariably based on economics. Once downhole activities or production is discontinued, well status needs to be distinguished between: *suspension*,

temporarily abandoned, or *permanently abandoned* (*NORSOK D-010 2013; Oil & Gas UK 2012a*).

Suspension is a well status where the activities on an under construction or intervention well are suspended. The operation may be suspended without removing the well control equipment. Reasons for suspension may be but not limited due to wait on weather, wait on a workover, wait on equipment, rig skidded to do short-term work on another well, for batch drilling (top section of hole only) (*Abshire et al. 2012; Barclay et al. 2001*).

Temporarily abandoned is a well status where the well is abandoned and/or the well control equipment is removed with the intention of re-entry or permanent abandonment at a later time. It could be said that temporary abandonment is a long-term suspension. Temporary abandonment could occur during a long shut-down while waiting on a workover or waiting on field development or re-development (*Abshire et al. 2012; Barclay et al. 2001*). Temporary status should begin the day after the completion has been isolated from the wellbore and may take from days up to several years. Different regulatory bodies have their own requirements with respect to the maximum period of temporary abandonment.

Permanently abandoned is a well status where the well or part of the well has been permanently plugged and abandoned with the intention of neither re-use nor re-entry. A well may be permanently plugged and abandoned due to end of current economic production, a well problem that cannot be economically repaired, or slot recovery operation. Exploration wells are usually permanently plugged and abandoned after information gathering. Once individual wellbores have been permanently plugged and abandoned, the pipelines, facilities, and other structures in the field must be decommissioned and removed (*Abshire et al. 2012; Barclay et al. 2001*).

1.4. The North Sea Regulatory Authorities

Regardless of temporary or permanent abandonment, operators must leave behind a wellbore that is secured in accordance with local regulations. **Fig. 1.2** illustrates some regulatory authorities who survey petroleum activities in their own region. Different regulatory bodies have their own requirements and operators must strictly adhere to local well abandonment regulations. Usually, local regulations are the minimum requirements and have changed considerably over the years to facilitate P&A operations safely. Nevertheless, some operators also have their own internal standards and tend to follow them where the regulatory authorities do not provide minimum standards.

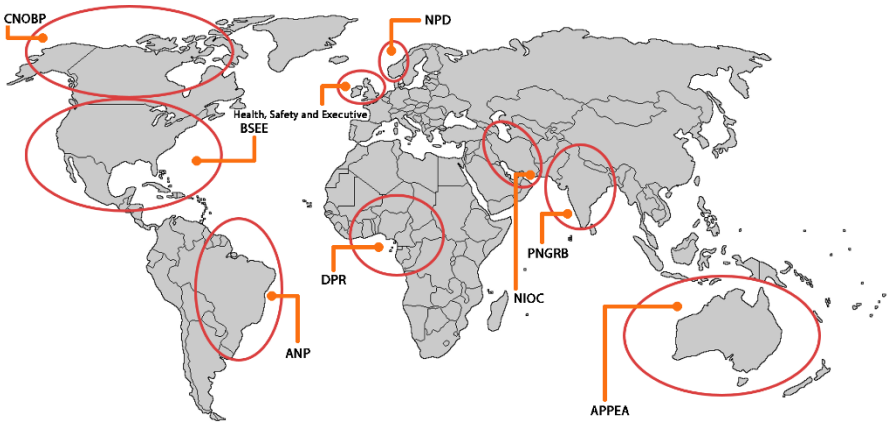

Figure 1.2 Regulatory authorities that survey petroleum activities within their jurisdiction.

The North Sea is divided into four sectors: the United Kingdom, Norwegian, Danish, and Dutch (*Liversidge et al. 2006*). The Health and Safety Executive is the appropriate department that oversees the petroleum activities in the UK sector. In the Danish sector, the Danish Energy Agency (DEA) is the regulatory authority. The Dutch Supervision of Mines and the Norwegian Petroleum Directorate (NPD) are the regulatory authorities for the Dutch and Norwegian sectors, respectively (*Fronks 2002*). NPD is the governmental specialist

directorate and administrative body for the NCS. NPD acts as an adviser to the Ministry of Petroleum and Energy (MPE) of Norway.

In the Norwegian maritime territory, an independent government regulator known as the Petroleum Safety Authority (PSA) has responsibility for safety and emergency preparedness in the Norwegian petroleum industry. The PSA is the legislated authority for P&A activities, reviews proposed P&A plans on the NCS, and is the responsible for surveying P&A operations.

1.4.1 The North Sea Regulatory Abandonment Requirements

P&A projects in the North Sea are designed mostly in accordance with the guidelines and the standards issued by the government and/or operator associations. Well integrity in drilling and well operations, widely known as *NORSOK D-010* standard (*2013*), is the standard for P&A operations in the Norwegian sector. Similarly for the UK sector, the guidelines are set in the *Guidelines for Suspension and Abandonment of Wells* (*2012a*) and for the Netherlands sector in the *Mining Act of the Netherlands* (*Liversidge et al. 2006*). All the standards and guidelines are essentially along similar lines and aim for the prevention of:

- hydrocarbon and water leakage to the surface,
- hydrocarbon movement between different strata,
- contamination of water-bearing zones, and
- pressure breakdown (fracture initiation) of shallow formations.

1.5. Well Barriers

To plug a well, regardless of the P&A type, a well barrier is necessary to be established preventing fluid(s) from flowing unintentionally. A well barrier is an envelope of one or several dependent well barrier elements. A well barrier element is a physical element which in itself may not prevent flow but in combination with other well barrier elements creates a well barrier (*NORSOK*

D-010 2013), as shown in **Fig. 1.3**. Any object or device that blocks a hole or a passage is defined as a plug. Plugs may be considered a part of well barrier elements and can be divided into two categories: *mechanical plugs* and *non-mechanical plugs*. A mechanical plug is a device used to create a seal inside the casing. It is important to note that mechanical plugs are considered neither well barrier elements nor well barriers for permanent P&A. However, they are considered well barriers for temporary P&A. It should be emphasized that mechanical plugs may be utilized as a foundation for permanent non-mechanical plugs to minimize contamination and improve the quality of permanent plugs.

Non-mechanical plugs, plugging materials, can be divided into different categories such as cementitious, grouts, thermosetting polymers and composites, thermoplastic polymers and composites, and formation. Portland cement is an example of a sub-group of the cementitious materials (*Oil & Gas UK 2012b*).

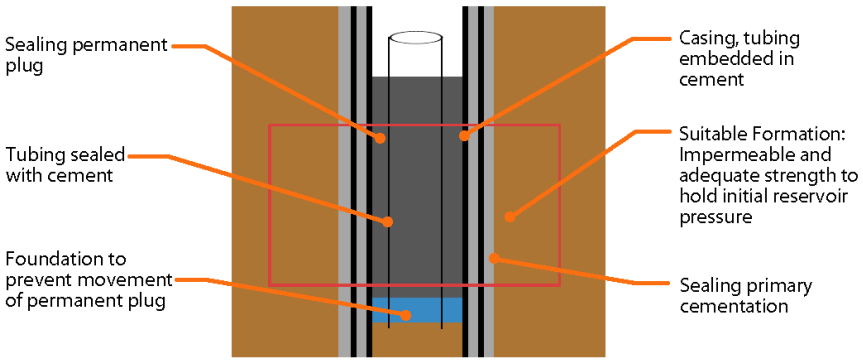

Figure 1.3 Well barrier elements of a permanently abandoned cased hole.

1.5.1. Well Barrier Requirements for P&A

In P&A operations, two well barrier envelopes are necessary to be assigned: *primary well barrier* and *secondary well barrier*. A primary barrier is the first set of barrier elements above the point of potential inflow. A secondary barrier

is a backup for the primary barrier and shall fulfil all the requirements of the primary barrier (*NORSOK D-010 2013*). If the well barriers are established with the purpose of a temporary abandonment, they are termed as *primary and secondary temporary barriers*. Otherwise, they are established for permanent abandonment and are called *primary and secondary permanent barriers*. It is essential to establish primary and secondary well barriers for both temporary and permanent abandonment to control the flow of unwanted fluids. However, if the source of potential is a water-bearing zone with normal pressure, then one barrier is acceptable (*NORSOK D-010 2013*).

1.5.2. Openhole to Surface Well Barrier – Environmental Barrier

When the potential sources of flow are permanently secured, the permanent P&A operation is completed; however the PSA persuades operators to install an additional barrier to intercept link between the external environment and borehole. The plug is called *openhole to surface well barrier* or *environmental barrier* (*NORSOK D-010 2013*).

1.6. Suggested Characteristics for Permanent Plugging Materials

Different regulatory bodies have their own requirements for P&A operations. However, with respect to permanent barrier materials characteristics, the main characteristics should be the following: (i) provide long-term integrity, (ii) have very low permeability or be impermeable, (iii) be non-shrinking, (iv) be ductile, (v) have resistance to downhole chemicals or substances (CO_2, H_2S, hydrocarbons, etc.), (vi) be able to bond to steel or formation, and (vii) be harmless to steel (*NORSOK D-010 2013; Oil & Gas UK 2012b*).

1.7. Cement as the Prime Material

Portland cement, subgroup of cementitious materials, is the prime material used in the petroleum industry both for sealing annular space between casing and

formation and zonal isolation. Experimental and numerical work performed by Andrade (*2015*) shows that casing centralization, rock formation type, casing surface condition, and thermal cycling impact cement-sheath integrity. There are some liabilities regarding the chemical and physical properties of Portland cement during and after hardening such as chemical and autogenous shrinkage, possible gas influx (permeability), long-term durability issues, and instability at high temperatures in corrosive environments (*Satoh et al. 2013; Chartier et al. 2008; Reddy et al. 2009; Gherardi et al. 2012*). Therefore, there is a need for alternative materials to minimize such concerns.

1.8. *Objectives of the Thesis*

Guidelines on qualification of materials for the suspension and abandonment of wells (*Oil & Gas UK 2012b*) categorizes materials that may be suitable for a permanent well barrier into nine types. The categorization is based on the chemical and physical nature of available materials. Geopolymers are one example of cementitious materials.

Since geopolymers have shown outstanding properties such as, it is of importance to investigate their applicability as an alternative to Portland cement for permanent P&A. Therefore, the current work investigates some of the fundamental properties and functional requirements that a plugging material should possess (*Oil & Gas UK 2012b*).

Chapter 2

Geopolymers

2.1. Historical Overview of Alkali Activated Binders

Modern usage of geopolymers started with the application of blast furnace slag. The synthesis of construction materials by alkaline activation of high-calcium blast furnace slag was first demonstrated by Purdon in 1940 (*Provis and Deventer 2009*). In 1959, Gulkhovsky established the theoretical basis and development of alkaline cements; thus introducing the term '*alkaline cements*' in 1965 (*Pacheco-Torgal et al. 2015*). In the 1970s, Davidovits introduced the term '*geopolymer*' by presenting the concept of mineral polymers (*Davidovits 2011*). Now a question arises and that is, what is the difference between the terms 'alkaline cements' and 'geopolymers'?

The main difference between 'alkaline cements' and 'geopolymers' is initiated from the chemical composition of the starting material and alkaline concentration. The calcium content of the source material is the key element that influences the required concentration of alkaline solution. Generally, alkaline cements are produced from high-calcium content materials with of lower concentrations of alkaline solutions which yield calcium aluminosilicate hydrate (C-A-S-H) gels. While, geopolymers are formed from low-calcium content materials with a need of higher concentrations of alkaline solutions (*Provis and Deventer 2009*; *Pacheco-Torgal et al. 2015*; *Davidovits 2011*).

2.2. Geopolymers

Geopolymers are alternative cementitious materials synthesized by combining source materials that are rich in silica and alumina with strong alkali solutions.

In other words, geopolymers are solid and stable aluminosilicate materials formed by the activation of a source material using an activator. The source material is a low-calcium content aluminosilicate substance, where the aluminosilicates are in a tetrahedral framework with negative charges on the edges, **Fig 2.1**. If the aluminosilicates do not contain negative charges, they need to be activated (*Ferone et al. 2015*).

a) b)

Figure 2.1 Tetrahedral frameworks of silica and aluminosilicate, a) Orthosiloxonate, b) Tetrahedral configuration of sialate.

In order to produce a geopolymer, starting material (powder) is mixed with an activator. The activator could be an alkali hydroxide, alkali silicate solution, or a combination of both. The reaction yields an inorganic material, a geopolymer, with favorable chemo-physical properties. A variety of aluminosilicate materials have been suggested to be used as solid raw materials for geopolymerization: fly ash, metakaolin, palm oil fuel ash, rice husk ash, red mud, and naturally-occurring minerals (*IV; Davidovits 2011; Singh et al. 2015; He et al. 2013*).

2.2.1. Reaction Mechanisms

Although the detailed chemical reaction that yields geopolymers is not fully understood, a three-stage conceptual mechanism has been proposed (*Provis and Deventer 2009*; *Pacheco-Torgal et al. 2015*; *Davidovits 2011*): a)

depolymerization of oxide minerals from source materials; b) transportation/orientation of dissolved oxide minerals; and c) polycondensation to form 3D networks of aluminosilicate structures.

a) Depolymerization

The reaction commences with the attack of OH^- ions present in the alkaline solution to the $\equiv Si - O - Si \equiv$ bonds. The ions redistribute the electron density around the silicon atoms. Therefore, the silicon atom becomes unstable and the bonding between the silicon and oxygen may rupture (see Eq. 2.1). This reaction yields silanol ($\equiv Si - OH$) and sialate ($\equiv Si - O^-$) species.

$$\equiv SiO - O - Si \equiv + OH^- \rightarrow \equiv Si - OH + \equiv Si - O^- \quad (2.1)$$

The OH^- ions attack the $\equiv Si - O - Al \equiv$ in the same way (see Eq. 2.2).

$$\equiv SiO - O - Al \equiv + OH^- \rightarrow \equiv Si - O^- + \equiv Al - OH \quad (2.2)$$

As the alkaline cations (e.g. Na^+, K^+) coexist in the medium, they neutralize the negative charges of the silate species and either postpone or prevent a return to the previous state of siloxane ($\equiv SiO - O - Si \equiv$). Moreover, the $\equiv Si - O^- Na^+$ complexes develop conditions for the transport of the reacting structural units and the creation of the coagulated structure. Therefore, the cations catalyze these reactions, whilst maintaining the ionic force needed to destroy the covalent bonds and consequently participating in the conversion of the destroyed bonds into a colloidal phase.

b) Transportation/Orientation

In this second stage, the depolymerized products, e.g. monomers, orient and due to the accumulation of other ionic species, the contact between the monomers increases. The increase in contacts ignites polycondensation.

Meanwhile, the silica monomers likely inter-act to form dimers (disiloxane) and in turn react with other monomers to build polymers. The transportation of monomers occurs in aqueous mediums and water acts as a carrier.

c) Polycondensation/Geopolymerization

In the final stage, geopolymerization takes place as a consequence of the interaction between the produced oligomers and the presence of particles in the initial solid phase.

It is noteworthy to mention that the OH^- ions act as catalyzer and the alkaline metal acts as a structural component by balancing the electronic charges. The aluminates also participate in the reaction by replacing the silicon tetrahedra during geopolymerization.

$$(HO)_3Si - O^- + (OH^-)_3 - Si - OH \rightarrow (HO)_3Si - O - Si - (OH)_3 + OH^- \rightarrow [(HO)_3Si - O - Si - (OH^-)_3]^- \quad (2.3)$$

Deventer *et al.* (*2007*) reported a post-reaction to the polycondensation, which happens quite slowly, that depends on post-synthesis treatment and the initial composition of the starting materials. The post-reaction, which is a part of the third stage, was termed '*Transformation*'. Transformation may cause a further crystallization and consequently can change the chemo-physical properties of the produced geopolymers. **Fig. 2.2** illustrates the simplified reaction processes involved in geopolymerization.

Based on the types of chemical bonding yielded as a result of the reactions, three types of structures can be derived from the 3D aluminosilicate network: poly(sialate) $(-Si - O - Al - O)$, poly(sialate-siloxo) $(-Si - O - Al - O - Si - O)$, and poly(sialate-disiloxo) $(-Si - O - Al - O - Si - O - si - O)$. The result of geopolymerization is a cementitious material with a high mechanical strength and high fire and acid resistance. In addition, geopolymers

are characterized by a number of physical characteristics including thermal stability, high surface smoothness, hard surface, long-term durability, and high adhesive property to natural stone and steel (*Provis and Deventer 2009*; *Pacheco-Torgal et al. 2015*; *Davidovits 2011*).

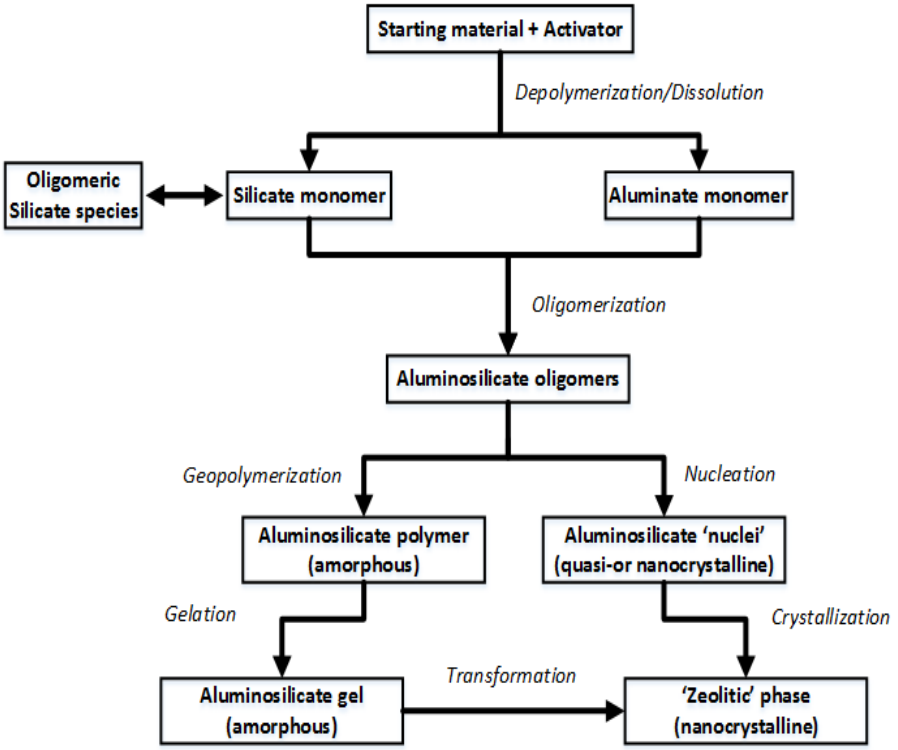

Figure 2.2 Illustration of reaction processes involved in geopolymerization (*Deventer et al. 2007*).

2.2.2. N-A-S-H (Sodium – Aluminosilicate – Hydrate) Gel Formation

Palomo proposed a two-stage model to describe geopolymerization (*Pacheco-Torgal et al. 2015*): a) nucleation and b) growth. Nucleation involves dissolution of aluminosilicates in an alkaline medium and polymerization of complex ionic species. This stage covers the first two stages of the reaction mechanism, which have formerly been reviewed (see section 2.2.1). Growth is

the second stage that takes place whenever the nuclei reach a critical size and crystals begin to grow. According to this model, the reaction yields a three-dimensional alkaline aluminosilicate hydrate known as N-A-S-H gel (*Garcia-Lodeiro et al. 2011*). These species have been suggested to have the following empirical formula (*Davidovits 2011*):

$$\{M_n(-(SiO_2)_z - AlO_2)_n \,.\, WH_2O\} \tag{2.4}$$

where *Z* is 1, 2, 3, or higher, *M* is a monovalent cation (e.g. Na^+, K^+), *W* number of water molecules, and *n* is a degree of polycondensation. This phase has been suggested to be formed likely in metakaolin-based and fly ash-based geopolymers (*Pacheco-Torgal et al. 2015; Davidovits 2011; Singh et al. 2015*).

It should be noted that the raw material and activator are not the sole elements that affect the structure of the N-A-S-H gel. Many other parameters, such as curing temperature and pressure, influence the physical properties of the final product.

2.2.3. Factors Influencing Geopolymerization

The geopolymerization process depends on many parameters including characteristics of raw materials (e.g. amorphous compound, chemical and mineralogical composition, particle size distribution or surface area, and Si/Al ratio) (*Nikolic et al. 2015; Ozer and Soyer-Uzun 2015; Fernandez and Palomo 2003*). Besides type and concentration of alkali solution, type and moduli of alkali silicate solution, alkali solution to alkali silicate ratio, curing pressure and temperature, water content, and curing time have been reviewed by different authors to have influence on the characteristics of geopolymers (*III; Kong and Sanjayan 2010; Zhang et al. 2014; Cheng et al. 2015*). These parameters can have significant influence on the rheological behavior, microstructure, mechanical properties, and long-term durability of geopolymers.

Chapter 3

Materials & Analytical Methods

In this chapter, materials and analytical methods used to develop, characterize, and investigate the applicability of geopolymers for oilwell cementing are presented.

3.1. Materials

3.1.1. Class C Fly Ash (CFA)

The used Class C Fly Ash (CFA) was fly ash used for concrete made in accordance with EN 450-1(*2012*) supplied by NorCem AS, Norway. The CFA has a higher calcium content compared to Class F. The pH of the used CFA in water was 12.1. The pH value was measured as described in section 3.3.8. **Fig. 3.1** shows element analysis and morphology of the CFA taken by Scanning Electron Microscopy (SEM) and Energy-Dispersive X-ray Spectroscopy (EDX).

3.1.2. Aplite Rock

Ground aplite rock was one of the materials used in this study to synthesize a rock-based geopolymer. The aplite rock was collected from Finnvolldalen, Namskogan, Norway. **Table 3.1** tabulates the chemical composition of the ground aplite rock provided by the supplier. **Fig. 3.2** shows element analysis and morphology of the aplite particle taken by SEM and EDX.

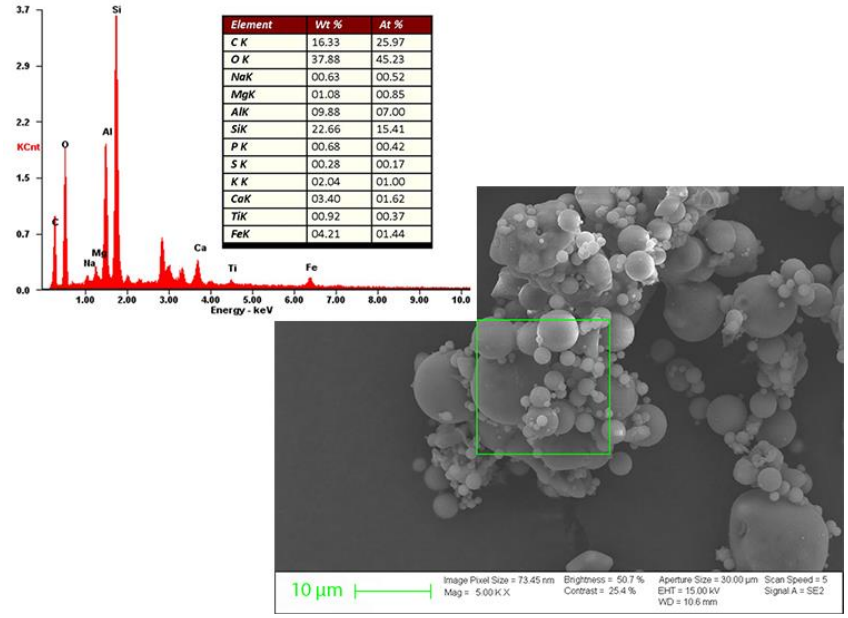

Figure 3.1 Element analysis and morphology of the CFA (*III*).

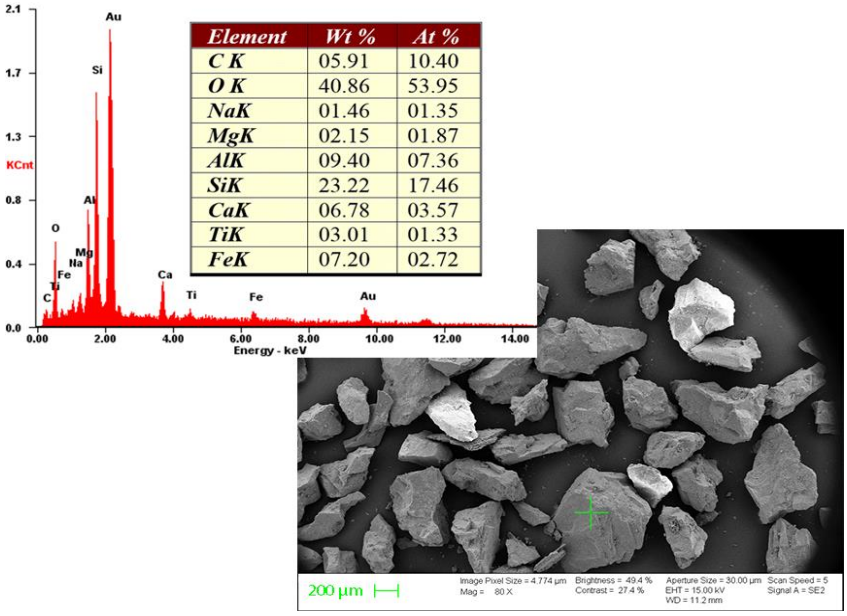

Figure 3.2 Element analysis and morphology of the aplite particle.

3.1.3. Microsilica

A highly reactive pozzolanic material, microsilica (Grade 995), was used as an additive in some mixes to increase the Si/Al ratio consequently synthesizing longer chains of geopolymers. **Table 3.1** shows the chemical composition of the microsilica supplied by Elkem AS, Norway.

3.1.4. Ground Granulated Blast Furnace Slag

An aluminum-, magnesium-, and calcium- rich Ground Granulated Blast Furnace Slag (GGBFS) from steel production was supplied by Merit 5000, Sweden. This material was used as an additive; the chemical composition is shown in **Table 3.1**.

3.1.5. Norite Rock

An anorthosite-like rock, mainly consisting of norite, and its chemical analysis were provided by Titania AS, as presented in **Table 3.1**. The norite-containing rock is one of the main waste tailings during the mining of ilmenite at the Titania AS mine in Sokndal, Norway.

3.1.6. Alkali Activator

Sodium hydroxide (NaOH) and potassium hydroxide (KOH) pellets were used for preparation of alkali solutions. They were caustic soda and caustic potash with 99% purity.

Sodium silicate solution, Na_2SiO_3, and potassium silicate solution, K_2SiO_3, were used in some mix designs. The Na_2SiO_3 was supplied by Merck KGaA, Germany and it is reported to contain 28.5% SiO_2, 8.5% Na_2O, and 63% H_2O. The K_2SiO_3 was supplied by Univar AS, Norway. The K_2SiO_3 contains 38% potassium silicate and 62% water.

3.2. Specimen Preparation

The geopolymers were prepared using both aplite and norite with different activators and different liquid to solid ratios (*II; III; IV; V; VI; VII; VIII*). The geopolymeric slurries were prepared in a WARING model 8009L commercial lab blender (*API 10B-2 2005*). Alkali solution was mixed with alkali silicate solution prior to adding the solid phases. The geopolymeric precursors were added during 50 seconds of mixing. The rotations used for mixing the components of the geopolymeric slurries were 4000 rpm for the first 15 seconds and 12000 rpm for the last 35 seconds, following the API10B-2 (*2005*) specification for well cementing.

To homogenize the slurry, it was poured into an atmospheric consistometer and mixed for 20 minutes at ambient conditions. In laboratory analysis of oilwell cement, this process is called '*pre-conditioning*' (*API 10B-2 2005*).

3.3. Analytical Method

3.3.1. Viscosity

A Chandler 35 rotational viscometer was utilized to measure the viscosity of the slurries in accordance with API 10B-2 (*2005*).

Table 3.1 Chemical composition of the used solid phased provided by suppliers.

Chemical (wt. %)	SiO_2	Al_2O_3	Fe_2O_3	CaO	MgO	Na_2O	K_2O	Cr_2O_3	TiO_2	MnO	P_2O_5	SrO	BaO	C	S^{-2}	Total	LOI
Aplite rock	82.8	9.04	0.75	0.82	0.1	2.72	3.11	<0.01	0.04	0.02	0.005	0.02	<0.01	-	0.00	99.45	0.29
Microsilica	95.5	0.7	0.3	0.4	0.5	0.4	1.0	0	0	0	0	0	0	1.0	0	99.8	2
GGBFS	34	13	0	31	17	0.9	0	0	2.4	0.6	0	0	0	0	1.1	100	-
Norite	43	15.5	12.5	6.6	6.8	3.4	0.9	0.03	8.2	6.8	0.3	0	0	0	0.1	97.43	2.57

LOI: Loss on Ignition

3.3.2. Thickening Time

To evaluate the thickening time of the mix designs, both pressurized and atmospheric consistometers manufactured by Chandler Engineering Company were used. The pressurized consistometer engaged Lab VIEW version 7.1 software to calculate the consistency in Bearden units of consistency. The atmospheric consistometer was equipped with a torque meter and a data acquisition system. The consistency in the atmospheric consistometer was calculated following Eq. 3.1.:

$$C = \frac{T-78.2}{20.02} \quad [\text{Bc}] \tag{3.1}$$

where T is the torque in (g.cm) and C is the consistency in Bearden units (Bc).

3.3.3. Strength Measurements

The strength of the cured material is the capacity of a material to withstand loads tending to reduce size. Some materials deform irreversibly at their strength limit and others fracture. The strength can be calculated in two ways: (i) compressive strength – measured by a crush test and (ii) sonic strength – compressive strength estimated ultrasonically.

3.3.3.1. Uniaxial Compressive Strength (UCS)

Generally, a uniaxial load is exerted on the surface of a specimen and measured continuously until the material fails completely. The instrument plots a stress–strain curve. The compressive strength is given by Eq. 3.2.

$$\sigma = \frac{F}{A} \tag{3.2}$$

where F is maximum applied force (N) and A is specimen surface area (mm^2). As the surface area of the specimen varies on compression and it is a function

of applied force, A = f(F). The original specimen area at the start of the experiment was used for the calculation.

For specimens with a compressive strength less than 500 psi, the loading rate of 1000 psi per minute was used. The specimens with a compressive strength greater than 500 psi experienced a loading rate of 4000 psi per minute, following the API 10B-2 (*2005*) specification for well cementing. The compressive strength of the geopolymers were measured by using a Toni Technik-H mechanical tester. The apparatus applies a TestXpert v7.11 testing software to determine the compressive strength.

3.3.3.2. Sonic Strength – Nondestructive Compressive Strength

Chandler Ultrasonic Cement Analyzers (UCAs) were deployed to estimate the sonic strength of the geopolymers at downhole conditions. A UCA consists of four main parts: (i) pressure vessel, (ii) heating system, (iii) pressure supplier, and (iv) data acquisition and control systems (**Fig. 3.3**). The UCA measures and records the ultrasonic travel time by using a Chandler 5270 Data Acquisition and Control System version 2.0.152. Normally a correlation is chosen from a library of available correlations based on the specific gravity of cement slurry. These are correlations that have been developed for cement slurries.

Figure 3.3 An Ultrasonic Cement Analyzer (UCA) with a pressure supplier.

As the common models have been generated for Portland cement and not geopolymers, the custom algorithm option in the UCA software was applied. To calculate the coefficients of the custom algorithm, polynomial equations were obtained by plotting transit time against measured compressive strength determined by crushing cylindrical specimens via the UCS tester.

3.3.3.3. Tensile Strength Measurements – Brazilian Test

To determine the tensile strength of the geopolymers, cylindrical specimens with certain dimensions (length = 2 × diameter) were placed between two pads in a mechanical tester (**Fig. 3.4**). The maximum applied force was recorded via a software and converted to tensile strength by applying the specimen dimension, Eq. 3.3.

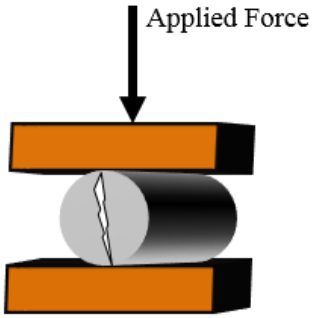

Figure 3.4 Pictorial representation of the tensile strength determination, Brazilian test.

$$\sigma_X = \frac{2F}{\pi DH} \tag{3.3}$$

where σ_x is tensile strength, F is maximum applied force to initiate the first crack (N), D is specimen diameter (mm), and H is length of specimen (mm).

3.3.3.4. Confined Triaxial Compression Measurements

Confined triaxial compression tests were performed in a hydraulic operated triaxial cell to measure the Bulk Modulus, Poisson's Ratio, Young's Modulus, Yield Strength, and creep at elevated pressures and temperature. So at time t=0, the confining pressure was increased to 0.5 MPa and the temperature increased to 90℃. The set-up was allowed to stabilize overnight. The next day, the confining pressure was increased hydrostatically to 15 MPa with a loading rate of 0.1 MPa/min. Thereafter, the confining pressure was kept constant at 15 MPa, and the axial stress was increased with the same loading rate (0.1 MPa/min) up to 21 MPa. After loading the specimen up to these stresses, the core was left to creep at constant stress for a minimum time of 7021 minutes.

Poisson's ratio (ν) (**Fig. 3.5**) is a measure of this effect and defined as the fraction of expansion divided by the fraction of compression. See for example

Aadnoy and Looye (*2011*) or Fjær *et al.* (*2008*). The Poisson's ratio is given by Eq. 3.4.

$$\nu = -\frac{\Delta r}{\Delta L} \tag{3.4}$$

where Δr is the changes in radius (mm) and ΔL is changes in length (mm). The Poisson's ratio is frequently considered during the material-design process.

Young's modulus or tensile modulus is a measure of the stiffness of an elastic material and is defined as the ratio of the stress along an axis to the strain along the same axis. **Fig. 3.6** shows a pictorial representation of the Young's modulus, E. Young's modulus characterizes the flexibility of a material. The Young's modulus is given by Eq. 3.5.

$$E = \frac{Stress}{Strain} = \frac{F/A}{\Delta L/L} \tag{3.5}$$

where F is the applied force (N), A is the surface area (mm^2), ΔL is the length changes (mm), and L is the initial length of the specimen (mm).

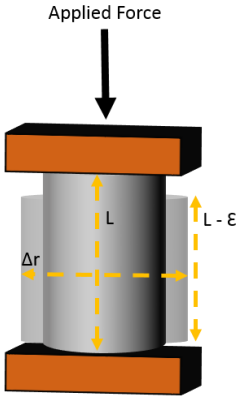

Figure 3.5 Pictorial illustration of Poisson effect on a cylindrical specimen caused by an exerted force.

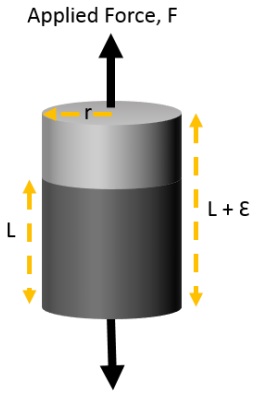

Figure 3.6 Young's modulus of a material.

The bulk modulus, Ƙ, measures the resistance of a material to uniform compression force, **Fig 3.7**. It is defined as the ratio of the infinitesimal pressure increase to the resulting relative decrease of the volume and given by Eq. 3.6.

$$K = -V\frac{dP}{dV} \tag{3.6}$$

where V is initial volume (mm^3), dP is differential pressure (Pa), and dV is changes in volume (mm^3).

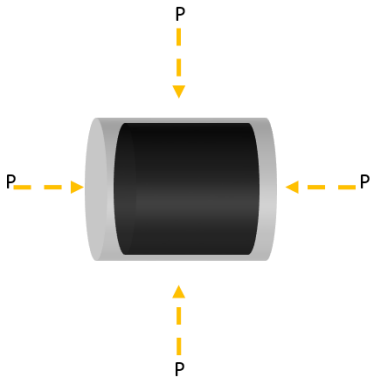

Figure 3.7 Bulk modulus of a material.

3.3.3.5. Mechanical Properties Analyzer

Mechanical Properties Analyzer (MPro) continuously measures the elastic mechanical properties of Portland cement under downhole conditions. The equipment measures both the compressional and the shear-wave velocities. It also estimates the elastic mechanical properties of the Portland cement from the velocities and the slurry density (*Nelson and Guillot 2006*). As the equipment has been designed for Portland cement, a modification was necessary to be done on its firmware to make it ready for the geopolymers.

3.3.4. Scanning Electron Microscopy

SEM is a type of electron microscope that uses a focused beam of high-energy electrons to generate a variety of signals at the surface of solid samples by scanning. **Fig. 3.8** shows the SEM instrument used to study the morphology and analyze the elements of particles. It mainly consists of an electron column, a sample chamber, an EDS (Energy-Dispersive X-ray Spectroscopy) detector, an electronic console, and visual display monitors.

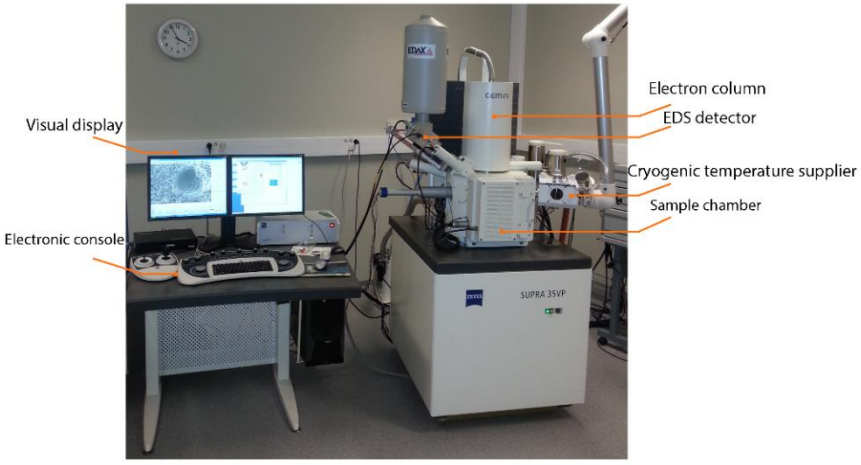

Figure 3.8 The SEM used in this study.

Generally, the emitted beam of electrons interacts with atoms at the surface of the sample and consequently produces various signals. The produced signals are detected and they contain information about the topography (texture) of the sample's surface and its chemical composition.

3.3.5. X-Ray Diffraction

The human eye can detect only a narrowband of electromagnetic radiation of light without additional aid. Electromagnetic radiation has a spectrum that goes far beyond the familiar color of the rainbow, **Fig. 3.9**. This concept has been

expanded greatly to comprise any interaction with radiative energy as a function of its wavelength or frequency.

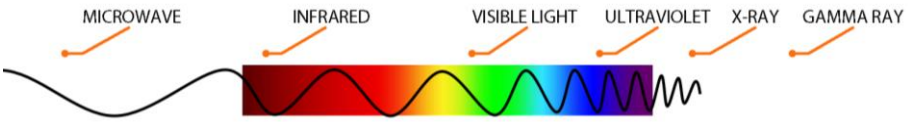

Figure 3.9 The electromagnetic spectrum of light.

The application of X-rays to the study of materials has probably been one of the most important, powerful, and widely-used analytical techniques available to material scientists. Clearly, this technique affected the study of crystalline minerals as well. Chemical, physical, and optical properties of crystalline minerals indicate that their structures consist of regular and repeating arrays of atoms, though, they cannot illuminate these structures directly. Study of the interaction of X-rays with mineral structures can allow determining the detailed arrangement of atoms.

3.3.5.1. X-rays

X-rays are waves of electromagnetic radiation similar to light waves, **Fig. 3.9**. X-rays are part of the electromagnetic spectrum whose wavelengths are between 0.1 and 10Å. X-rays are generated when a stream of electrons strikes the atoms in a metal or is being accelerated. The wavelength(s) of X-rays depends both on the energy of the electrons and nature of the metal that they strike (*Nesse 2000*). When the electron hits the target, X-rays can be created by two different atomic processes: (i) Characteristic X-ray or (ii) Bremsstrahlung/Synchrotron radiation. The Synchrotron radiation technique is only reviewed here as it has been used in this study to characterize the geopolymers.

3.3.5.2. Synchrotron Radiation/Bremsstrahlung

When a charged particle is accelerated, it emits radiation. The acceleration can be brought about either by the interaction with the charge of the nucleus of a metal (anode) or it can be induced by permanent magnets of an electron beam.

In the synchrotron scenario, the electromagnetic radiation is emitted when charged particles are accelerated radially. The synchrotron radiation is generated by the centripetal acceleration of either relativistic or ultra-relativistic charged particles in magnetic fields. The magnetic field is usually generated by using permanent magnets. **Fig. 3.10** illustrates the principal of the synchrotron radiation.

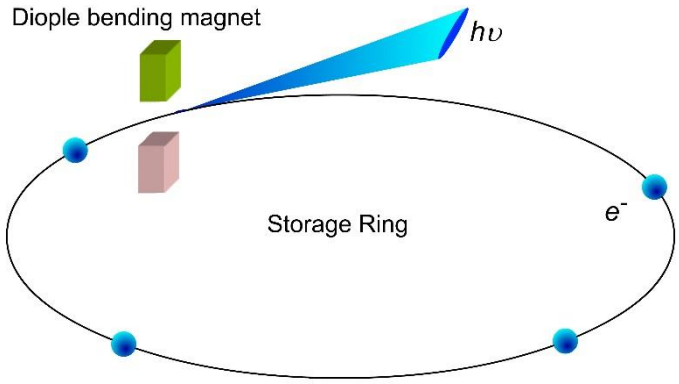

Figure 3.10 The principal of the Synchrotron X-ray generation.

3.3.5.3. X-ray Powder Diffraction of Minerals

X-rays are used to explore microscopic and atomic structures of matter. In X-ray crystallography, a beam of X-rays interact with the electrons of atoms within the sample. The powdered sample consists of small crystals. The X-rays either can pass through or be reflected by the planes of atoms within the crystals. The reflected X-rays follow the laws of reflections; the angle of incidence is equal to the angle of reflection from surfaces. The law of reflection is applied equally if the surface is discontinuous, as a surface made of layers of

atoms. In other words, each layer of atoms in the surface is capable of reflecting the beam of X-rays, **Fig. 3.11a**.

As the X-rays are waves, they should be added up. The scattered X-rays can be in phase, which means all the peaks and troughs of X-rays are lined-up (**Fig. 3.11b**). Consequently, the constructive interference will result in a wave with a higher amplitude. As shown in **Fig. 3.11b**, the scattered beam of X-rays from the lower layer of atoms needs to travel an additional distance compared with the scattered X-ray of the upper layer. This is shown with two dark arrows in **Fig. 3.11b**. If the diffracted X-rays are not in phase, the additional distance is not an integer number of wavelengths, the peak of wave 1 aligns with the trough of wave 2 (**Fig. 3.11c**). In this situation, these two waves cancel each other out and as a result, no scattering will be detected. Therefore, the angle of incidence should be selected correctly; otherwise, no scattering will be detected. By recording the diffraction angle, θ, with a well-known X-ray wavelength, λ, the distribution of interplanar distances, d, for different sets of parallel planes may be mapped out. This set constitutes the "fingerprint" of the actual mineral phase presented in a sample (*Waseda et al. 2011*).

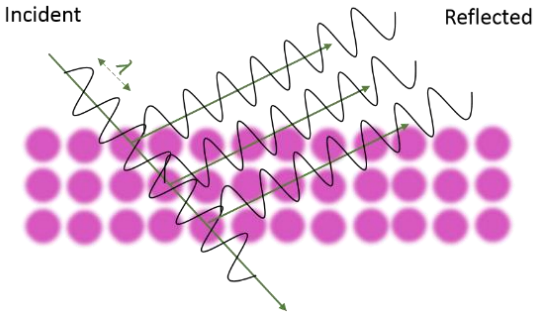

a) Atomic-scale crystal lattice planes.

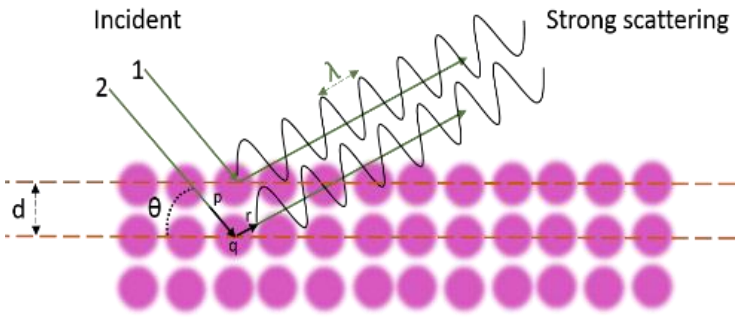

b) The diffracted X-rays exhibit constructive interference when the additional distance is an integer number of wavelengths.

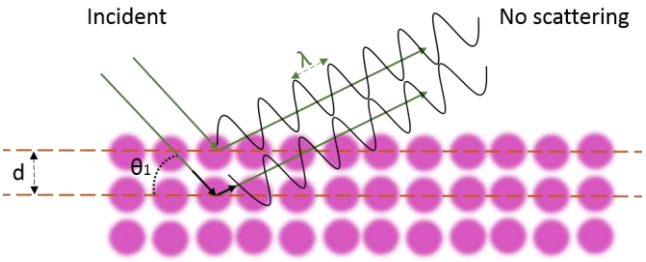

c) The diffracted X-rays exhibit destructive interference when the additional distance is not an integer number of wavelengths.

Figure 3.11 X-ray diffraction from parallel atomic planes.

Identification of crystalline minerals is routinely performed with the powder diffraction method. In this method, the sample is ground to powder where small crystals are assumed to be randomly oriented relative to each other. The X-ray beam hits the sample within a suitable range of angles and X-ray patterns are produced by the diffraction of X-rays through the closely spaced lattice of atoms within a crystal. The patterns are analyzed to reveal the nature of that lattice (d-spacing distribution). Then, a computer processing takes place for phase identification. The 2D pattern is transformed to a 1D curve with peak(s) through an azimuthal integration. Each peak represents minerals at certain angles. Finally, a phase-matching comparison to a database of known mineral

structures is done to identify unknown phases (*Hammersley et al. 1996*), as shown in **Fig. 3.12**.

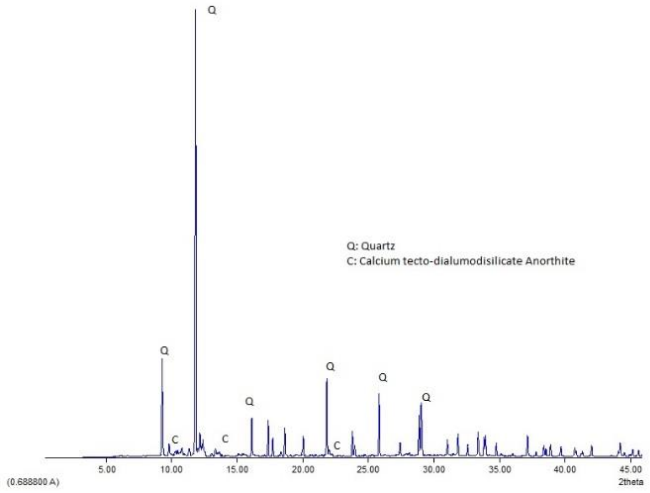

Figure 3.12 X-ray pattern of the ground aplite (Fig. 3.11a). Some peaks have been identified by matching. The background is almost flat, which shows that the sample is mainly crystalline (*IV*).

3.3.6. Shrinkage Measurements

The material balance technique was employed to measure the bulk shrinkage factor of the specimens while at a desired pressure and temperature setting. In this method, the slurry must be designed not to set prior to achieving Bottom Hole Circulating Temperature (BHCT). The designed slurry was poured into a High Pressure – High Temperature (HPHT) plastic balloon with determined weight. The balloon is placed inside a core holder and this is filled with tap water. The core holder is equipped with two valves; one is connected to a chromatography pump and the other one is connected to a pre-adjusted relief valve. The core holder is placed inside a heating cabinet to provide the BHCT. **Fig. 3.13** shows the schematic of the used set-up. When the geopolymeric material is set, the valves are closed and the core holder is disconnected. The

core holder is weighed by using a scale and it is connected to the system again. The pressure is increased by injecting water to compensate the dropped pressure caused by shrinkage of material and some time is given to stabilize the pressure and temperature. The core holder is disconnected again and weighed. Eqs. 3.7 and 3.8 were used to estimate the bulk shrinkage factor (SF).

$$V_2 = \frac{(m_2 - m_1)}{\rho} \tag{3.7}$$

$$SF = \frac{(V_1 - V_2)}{V_1} \tag{3.8}$$

where m_2 is mass of the core holder at step 2 (g); m_1 is mass of the core holder at step 1 (g); ρ is the water density at BHCT and aim pressure (g/cc); V_2 is volume of the injected water (cc); V_1 is the volume of designed slurry at the BHCT and aim pressure prior to setting. The balloon should be impermeable to prevent water penetration into the specimen.

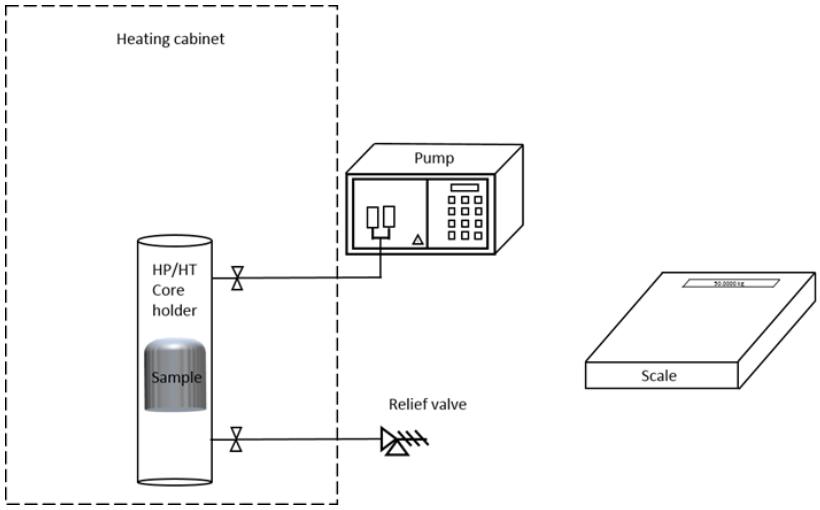

Figure 3.12 Illustration of HPHT shrinkage measurement setup.

3.3.7. Permeability Measurements

A coreflooding setup was used to measure permeability of the geopolymers. A QX series of Quizix pump was used to increase the overburden pressure to 24 MPa [3480 psi] and inject distilled water at a constant pressure of 21 MPa [3045 psi]. As the permeability was very low, the outlet pressure was selected to be ambient. The experiments were performed at ambient temperature.

3.3.8. pH Measurements of the Solid Materials

The pH values of the geopolymers were measured after setting, whereby, the set geopolymers were powdered by using a Retsch PM100 grinder at 356 rpm for 10 min. 5 g of the powder was mixed with 50 g of deionized water. Finally, the pH was measured after 5 min of mixing.

Chapter 4

Results and Discussion

4.1. Rheological Determination

4.1.1. Viscosity

Viscosity is a measure of the resistance of a material to deform irreversibly when exposed to an external force. This behavior is a result of internal friction in the material. Solid/liquid content, temperature, curing time, shape of solid phase(s), type of alkali hydroxides, type of alkali silicate solution, and water content have influence on viscosity of geopolymers (*Romagnoli et al. 2012; Puertas et al. 2014*). **Fig. 4.1** shows the shear stress vs. shear rate of sodium containing (Na-containing) and potassium containing (K-containing) geopolymers. Although the yield stresses were approximately equal, 3.8 Pascal, Na-containing systems show markedly higher viscosity than K-containing systems (*IV; Provis and Deventer 2009*). **Fig. 4.2** shows the shear rate vs. shear stress of the fly ash- and aplite- based geopolymers. The higher shear stress of the fly ash-based geopolymers could be due to either the particle size distribution, inter-particle distance or the particle geometry.

A non-Newtonian behavior for geopolymeric slurries have been observed and it has been suggested that geopolymers often follow the Bingham model (*IV; Criado et al. 2009; Pacheco-Torgal et al. 2015*).

Small yield stresses of geopolymeric slurries were noticed and reviewed by different authors (*VI; Pacheco-Torgal et al. 2015; Singh et al. 2015*). A small yield stress is preferable to reduce the particle segregation phenomenon in the event of a pump shutdown or during gelation.

4.1.2. Pumpability / Consistency

One of the prime challenges in the usability of geopolymer technology in the petroleum industry for oilwell cementing is the optimization for pumpability and strength development. **Fig. 4.3** shows the pumpability of aplite-based geopolymers with different mix ratios. Besides changing the mix ratio, retarder could be used to prolong the pumpability of geopolymers. **Fig. 4.4** shows that the addition of increasing amounts of sucrose efficiently increases the pumpability time for 30 Bc. Rattansak *et al.* (*2011*) studied the effect of sucrose as a retarder on high-calcium fly ash-based geopolymers. They concluded that the addition of 1.0 wt. % of sucrose to the geopolymer mixture delayed the setting time and enhanced the strength.

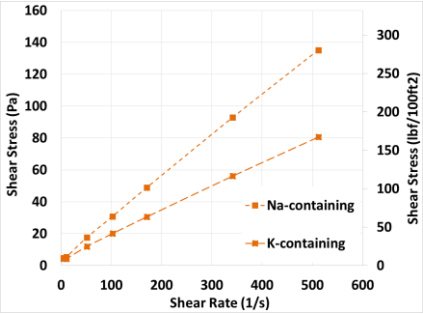

Figure 4.1 Shear stress vs. shear rate for Na- and K- containing aplite-based geopolymers at ambient condition (*IV*).

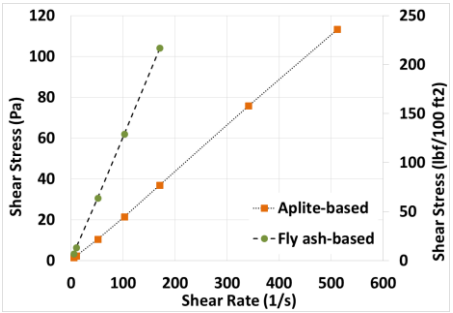

Figure 4.2 Shear stress vs. shear rate for fly ash- and aplite- based geopolymers at ambient condition (*III*).

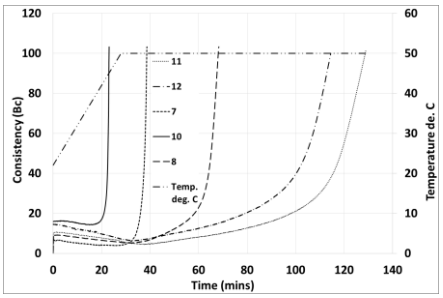

Figure 4.3 Atmospheric consistometer of the aplite-based geopolymers with different mix ratios at 50℃ (*V*).

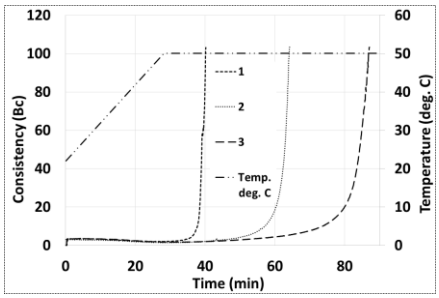

Figure 4.4 Atmospheric consistometer of the aplite-based geopolymers with different dosages of retarder at 50℃ (*VI*).

4.2. Physical Observation

Color changes of a geopolymeric material could be a chemical indicator of geopolymerization progress (*Davidovits 2005*). **Fig. 4.5a** shows the aplite-based geopolymer cured at ambient condition for 7 days. **Fig. 4.5b** and **Fig. 4.5c** show the color changes of aplite-based geopolymer after 7 days and 365 days of curing at 87℃ and ambient pressure. All the specimens were cured in molds of 52 mm diameter.

Proper curing condition has been shown to influence the mechanical properties of the aplite-based geopolymers significantly. **Fig. 4.5a** shows the aplite-based geopolymer, which was subjected to air during curing. As illustrated, some cracks appeared on the upper side of the sample. However, this phenomenon was not observed for the samples, which were sealed during curing in a plastic mold. One reason could be the evaporation of the water, which are either physically bonded or as hydroxyl groups (*IV; Salih et al. 2015*).

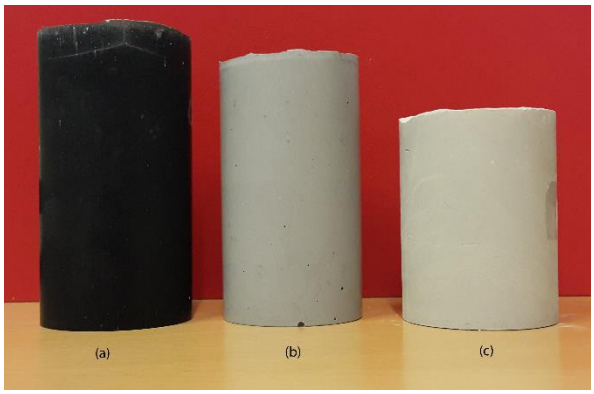

Figure 4.5 Color changes of the aplite-based geopolymers; (a) cured at ambient pressure and temperature for 7 days, (b) cured at 87℃ and ambient pressure for 7 days, and (c) cured at ambient pressure and 87℃ for 365 days.

4.3. Uniaxial Compressive Strength

Compressive strength development of geopolymers is a function of many parameters such as Si/Al ratio and calcium content of the starting material, type and concentration of alkali solution, type and moduli of alkali silicate solution, surface area of the particles in the starting materials, curing temperature, liquid/solid ratio, and water content as studied and reviewed by different authors (*Singh et al. 2015; Jang and Lee 2016; Hwang and Huynh 2015; Salih et al. 2015*). **Fig. 4.6** shows the effect of curing temperature on the compressive strength development of fly ash-based geopolymers. As the temperature increases from 87 to 125℃, it seems that a consecutive reaction takes place after 1 day of curing and retrogrades the compressive strength. This phenomenon became more vigorous when the concentration of NaOH was increased (**Fig. 4.6b**). The reason for this phenomenon remains unclear.

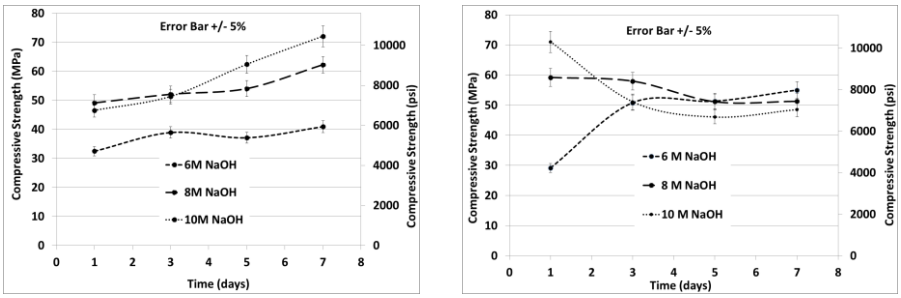

(a) Fly ash-based geopolymers cured at 87℃ and 5000 psi (*II; III*).

(b) Fly ash-based geopolymers cured at 125℃ and 5000 psi (*II; III*).

Figure 4.6 Effect of curing temperature on the compressive strength development of the fly ash-based geopolymers.

Fig. 4.7 shows the compressive strength development of the aplite rock-based geopolymers cured for 28 and 56 days at ambient pressure and 87℃. The higher the concentration of the alkali solution, the higher the compressive strength (*Hounsi et al. 2014; Yusuf et al. 2014*). However, this study showed that the effect of the type of alkali silicate solution and alkali solution to alkali silicate solution ratio influences the compressive strength substantially (*IV*). Based on the obtained result, the mixture prepared with 4M KOH solution showed higher compressive strength compared to the 6M KOH solution mixture, **Fig 4.7e**.

The obtained result in this study showed that the addition of sucrose as retarder up to 2 wt. % did not compromise the compressive strength (*VI*). **Fig. 4.8** shows that the addition of a proper amount of sucrose, 1 wt. %, slightly improves the compressive strength of the aplite-based geopolymers.

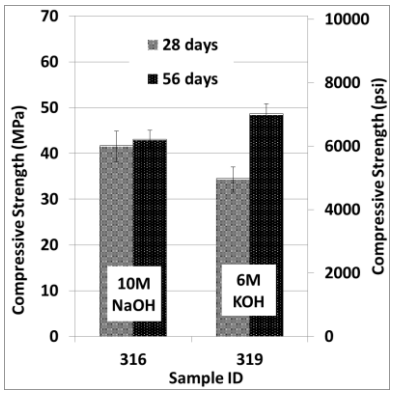

(a) Na-silicate solution to alkali solution ratio of 1.

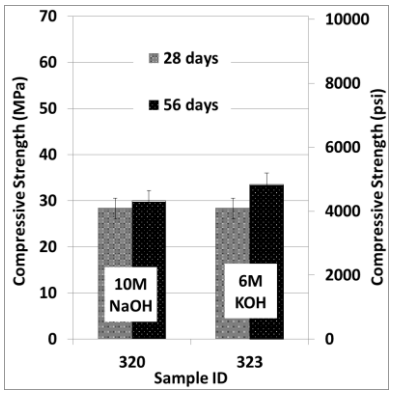

(b) Na-silicate solution to alkali solution ratio of 3:1.

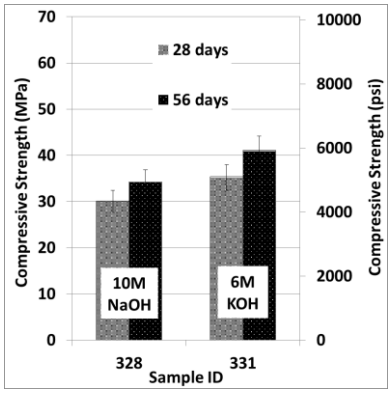

(c) K-silicate solution to alkali solution ratio of 1.

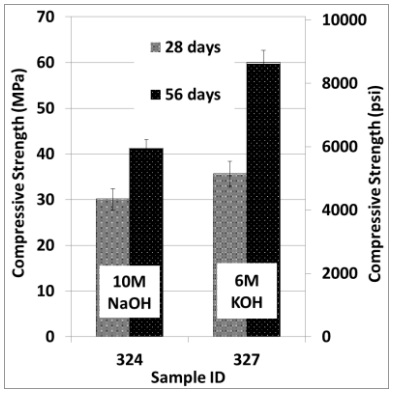

(d) K-silicate solution to alkali solution ratio of 3:1.

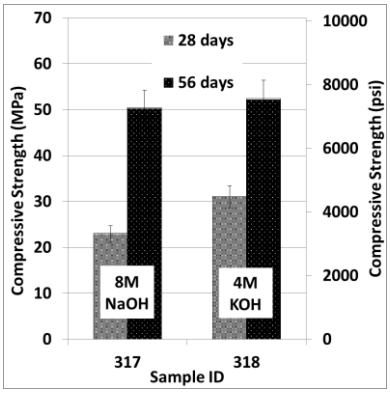

(e) Na-silicate solution to alkali solution ratio of 1.

Figure 4.7 Compressive strength development of the aplite-based geopolymers cured at ambient pressure and 87℃. Error bar shows +/- 5% of error (*IV*).

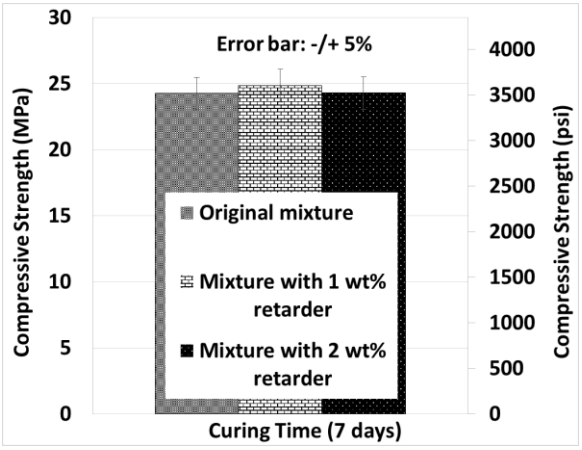

Figure 4.8 Uniaxial compressive strength of the aplite-based geopolymers cured at 90℃ and 2000 psi (*VI*).

4.4. Sonic Strength – UCA

UCAs are used in oil well cementing to estimate the sonic compressive strength of Portland cement. The obtained result showed that in order to use the UCAs for estimation of sonic compressive strength of geopolymers, the custom algorithm option should be activated. Consequently, algorithms were generated from the crushing tests (*API 10B-2 2005*) for each type of geopolymers with different activators and under different curing conditions as described in section 3.3.3.2 and in (*II; III*).

4.5. Confined Triaxial Compression Measurements

Dynamic mechanical properties of the geopolymers were measured by using two techniques: (a) using ultrasonic shear wave and compression wave combination measurements by deploying an MPro (*Reddy et al. 2005*) and (b) load vs. displacement technique, which is also known as triaxial compression measurements (*Fjær 2008*). **Tables 4.1** and **4.2** tabulate the bulk modulus, Young's modulus, and Poisson's ratio of the geopolymers measured by the two

techniques. **Table 4.1** presents the effect of changes of mix ratios and **Table 4.2** presents the effect of sucrose.

Table 4.1 Estimated dynamic mechanical properties of the aplite-based geopolymers at 87℃ and 1000 psi by using MPro (*V*).

Sample	Slurry Density (g/cc)	Poisson's Ratio	Bulk Modulus (kpsi) [GPa]	Young's Modulus, E (kpsi) [GPa]
7	1.90	0.28	746 [5.14]	1063 [7.33]
8	1.93	0.15	404 [2.78]	107 [0.74]
9	1.89	0.28	1057 [7.28]	1371 [9.45]

Table 4.2 Measured dynamic mechanical properties of the aplite-based geopolymers at 90℃ and 2000 psi by using triaxial compression cell (*VI*).

Mix design	Bulk modulus (kpsi [GPa])	Young's modulus (kpsi [GPa])	Poisson's ratio	Axial creep (%) [t=7021 min]	Radial creep (%) [t=7021 min]
1	241.0 [1.66]	207.2 [1.43]	0.016	2.09	0.86
2*	222.3 [1.53]	238.0 [1.65]	0.015	2.00	0.88
3	221.2 [1.53]	213.1 [1.47]	0.018	2.23	1.03

*Average values from two tests.

The measurements show that the addition of sucrose as retarder up to 2 wt. % of the total solid did not affect the dynamic mechanical properties of the geopolymers, **Table 4.2** mix design 3. However, the measured Poisson's ratios seem to be inconsistent with the estimated dynamic mechanical properties obtained from MPro, **Table 4.1**. One possible reason could be that these parameters are time-dependent parameters.

The study conducted by Nasvi *et al.* (*2015*) on fly ash-based geopolymers shows that increasing confining pressure increased plastic deformation of their geopolymers.

4.6. pH Determination

The measured pH values, as described in section 3.3.8, for the fly ash-based geopolymers showed high values, 12.5, which could protect tubulars from

corrosion (*Davidovits 2011*). The obtained results show that pH value may change during curing time at elevated temperatures (*II; III*).

4.7. Shrinkage Determination

The chemical shrinkage of the aplite-based and fly ash-based geopolymers were measured at elevated temperature and pressure. A maximum value of 2% was measured (*V*). Deb *et al.* (*2015*) studied the drying shrinkage of fly ash-based geopolymers, which is due to evaporation of water. They discovered that an addition of GGBFS to the fly ash-based geopolymers reduced the drying shrinkage. It could be a reason for the aplite-based geopolymers, which were studied in this work. As GGBFS was blended with the ground aplite rock in the mix design.

4.8. Permeability Measurements

The permeability of geopolymers were measured by using a coreflood setup. The measured permeability of the geopolymers were in the range of nano-Darcy (*V*). Nasvi *et al*. (*2014a*) studied the permeability of class F fly ash-based geopolymers at different temperatures varying from 23 to 70 ˚C. Their result showed that the permeability of their geopolymers ranged from 0.0004 to 0.041 µD as a function of increasing temperature. Still the permeability did not deviate from the nano-Darcy range.

4.9. Effect of Curing Temperature

Curing temperature has a significant effect on the chemo-physical properties of geopolymers. Curing at elevated temperatures may increase the geopolymer strength at early age. However, the final strength of the samples cured at ambient temperature could be similar to ones cured at elevated temperatures (*Salih et al. 2015*). As was observed in this study, higher curing temperature of the mixes with the higher concentration of alkali solution may activate a

consecutive reaction, which could weaken the strength of the CFA geopolymers (*III*). Nasvi *et al*. (*2015*) observed that an increase of the curing temperature up to 60℃, increased the deviatoric strength of their fly ash-based geopolymers. However, above that temperature the deviatoric strength of their geopolymers decreased.

The result of our work showed that curing at elevated temperatures could slightly change the pH value of the fly ash-based geopolymers (*II; III*).

4.10. Effect of Alkali Solution

In some cases, the performance of the aplite-based geopolymers with lower concentration of alkali solution was superior to higher concentrations, **Figs. 4.7 a** and **e** (*IV*). In other words, by selecting the right activator, lower concentration or dosage of alkali solution yields an almost similar or in some cases even higher performance, **Fig. 4.7**.

The obtained results showed higher compressive strength for the specimens prepared by using K-containing systems than Na-containing systems (*IV; VII*). It has been reported that dissolution of aluminosilicate in sodium solution is more effective than potassium solution. However, the compressive strength of geopolymers is higher for the K-containing systems than the Na-containing systems (*Davidovits 2011; Ryu et al. 2013*).

4.11. Influence of Ground Granulated Blast Furnace Slag (GGBFS)

The effect of GGBFS on setting, pumpability, and early strength development of geopolymers has been studied and discussed by different authors (*Deb et al. 2015; Nath and Sarker 2014; Ravikumar et al. 2010*). It is believed that the addition of an amorphous silica phase leads to shorter setting time and higher compressive strength (*Deb et al. 2015*). The current work studied the influence of GGBFS on the compressive strength of norite-based geopolymers. Based on the obtained results, the addition of the GGBFS to the slurries, strongly affected

the compressive strength of the geopolymers cured at ambient pressure and temperature, **Table 4.3**. It could be said that to reach a higher compressive strength at lower temperatures, addition of GGBFS to the geopolymer mix could be an option (*VII*).

Table 4.3 Measured compressive strength of the norite-based geopolymers. The specimens were cured at ambient pressure (*VII*).

Specimen	norite (g)	GGBFS (g)	Alkali sol.	Wt. of alkali sol. (g)	K_2SiO_3 (g)	Na_2SiO_3 (g)	Curing Temp. (℃)	Curing time (day)	Compressive strength (±2 MPa)
2	183	91	8M NaOH	52	0	72	23	7	20
3	183	91	4M KOH	53	72	0	23	7	26
4	248	40	10M NaOH	61	61	0	87	1	5.0
4	248	40	10M NaOH	61	61	0	87	5	9.0
4	248	40	10M NaOH	61	61	0	87	7	9.0

4.12. X-ray Powder Diffraction

The crystallography of aplite- and norite-based geopolymers were studied by the X-ray powder diffraction technique. Quartz and calcium tecto-dialuminosilicate anorthite ($Al_2CaO_8Si_2$) were the main detected crystal phases of the ground aplite (*IV*). XRD patterns of the selected samples of aplite-based geopolymers showed quartz as the major phase and albite ($NaAlO_8Si_3$), microcline ($Al_{1.03}K_{0.986}Na_{0.014}O_8Si_{2.97}$), and stilbite-Na ($Al_{4.67}Na_{2.984}O_{36}Si_{13.07}$) as the minor phases (*IV*). Based on the obtained result, the increase of albite, and microcline phases in Na-containing systems may decrease the strength of aplite-based geopolymers and an increase of zeolite phase in K-containing systems may increase the strength development of the geopolymers (*IV*).

The XRD analysis of the ground norite showed that the starting material mainly consists of anorthite sodian ($Al_{1.52}Ca_{0.52}Na_{0.48}O_8Si_{2.48}$). Erionite, albite

and stilbite-Na were synthesized as a result of geopolymerization of the norite. Moreover, formation of an amorphous phase was noticeable in the norite-based geopolymers (*VII*). XRD patterns of the norite-based geopolymers showed that when norite was mixed with pure 8M NaOH solution, the amorphous phase content was increased (*VII*). The result of XRD analysis of norite-based geopolymers showed that K-containing systems had a lower content of amorphous phases compared to the Na-containing systems (*VII*).

4.13. Microstructure Characterization

Microstructure of the fly ash-, aplite- and norite- based geopolymers were studied. When higher concentrations of alkali solution, 10M NaOH, were used to produce the fly ash-based geopolymers, fly ash spheres were partly damaged. This damage was more noticeable at elevated temperatures and consequently the compressive strength of fly ash-based geopolymers decreased (*II; III*).

The SEM analysis of aplite-based geopolymers showed that the large particles do not participate in the reaction. However, the geopolymer binder keeps them tight within the bulk. **Fig. 4.9** reveals the SEM image of the aplite-based geopolymers. **Fig. 4.10** shows the (Backscattered Electron) BSE image and elemental EDX maps for the most abundant elements in the geopolymer.

The EDX analysis of norite-based geopolymers showed that the crystals mainly contain Si, Al, O, and Na. These elements could be representative of erionite and oligoclase as detected by XRD. The rhombohedral structure and spot element analysis of the rhombs suggest rhombohedron calcite (*Nesse 2000*). However, formation of rhombohedron calcite needs space and it is less likely to form inside the geopolymer matrix. Therefore, one possible reason could be the formation of the rhombohedrons only on the surface of the geopolymer matrix.

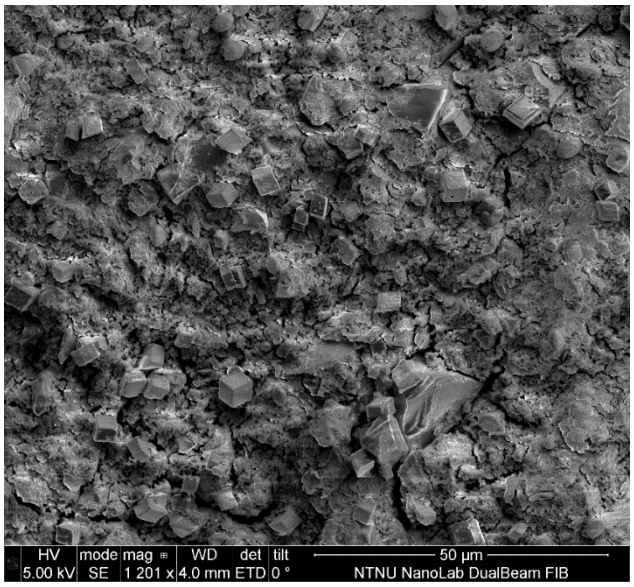

Figure 4.9 SEM image of the geopolymer prior to exposure.

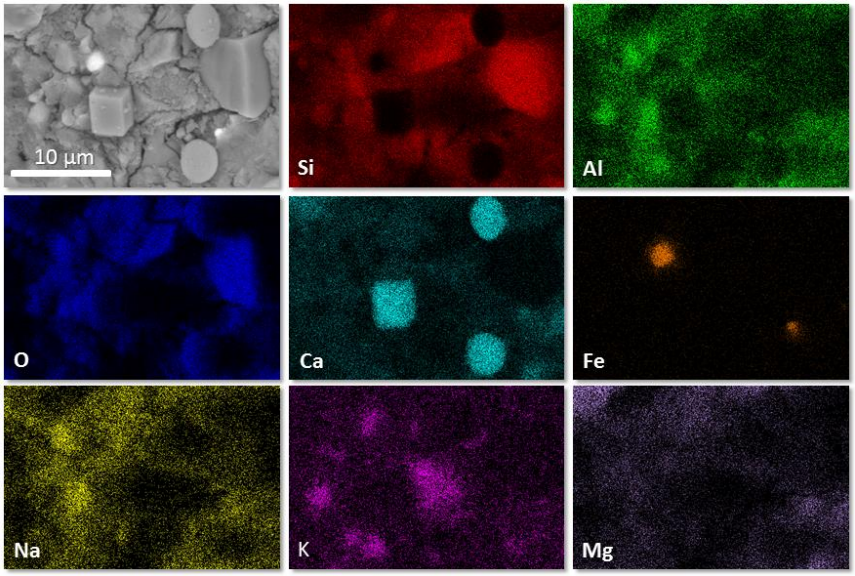

Figure 4.10 (Top left) BSE image and elemental EDX maps for the most abundant elements in the geopolymer: Si, Al, O, Ca, Fe, Na, K, and Mg (*VIII*).

4.14. Long-Term Durability

The long-term durability of the aplite rock-based geopolymers was examined at 100℃ with exposure to crude oil, brine, and H_2S in brine. In **Table 4.4** and **Fig. 4.11** are presented the results of compression tests. Exposure of the specimens to the brine showed a large variation in the compressive strength. A reduction in compressive strength up to 6 months of ageing was noticeable. However, the 12-month compressive strength of the specimens showed much the same of the initial specimens.

Table 4.4 Measured uniaxial compressive strength of the geopolymers aged at 100℃ (*VIII*).

	Initial strength (MPa) [psi]	1-month (MPa) [psi]	3-months (MPa) [psi]	6-months (MPa) [psi]	12-months (MPa) [psi]
Crude oil	66±5 [9570±725]	67±8 [9720±1160]	87±12 [12620±1740]	72*	86±14 [12470±2030]
Brine	66±5 [9570±725]	39±11 [5660±1600]	50±11 [7250±1600]	31±4 [4460±580]	69±19 [10010±2760]
H_2S	66±5 [9570±725]	48±5 [6960±725]	56±5 [8120±725]	46±5 [6670±725]	20±17 [2900±2465]

Average values and standard deviation from three specimens.
*Only one specimen measurable. The other two broken due to fracturing.

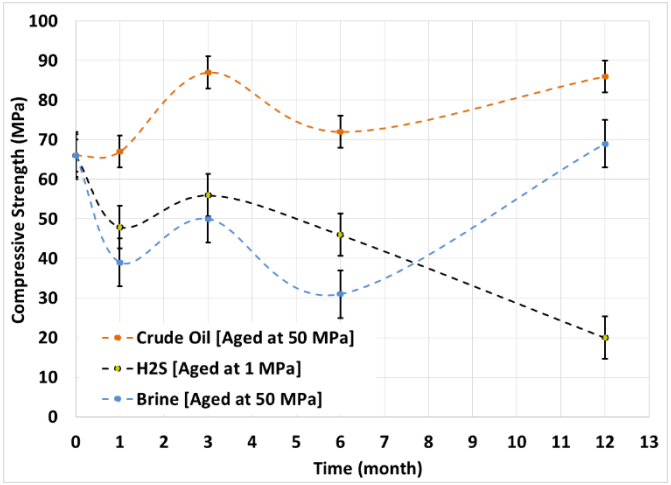

Figure 4.11 Compressive strength of the geopolymers, aged at 100℃ (*VIII*).

Nasvi *et al.* (*2014b*) studied the exposure of class F fly ash-based geopolymers to water and different salinities of brine to investigate their mechanical behavior. According to their findings, strength reduction rate of the

geopolymers decreases as the salinity of brine increases. They suggested that this is because when the water salinity increases, the alkali leaching rate decreases.

Exposure of the specimens to H_2S showed a continuous strength reduction of the geopolymers over time, **Table 4.5**. As the compressive strength of the geopolymers decreased over time, the variation in the measurement increased due to deterioration of the specimens in the corrosive environment. Unfortunately, no previous studies on geopolymers were found to discuss the result of H_2S exposure.

Table 4.5 Measured tensile strength of the geopolymers aged at 100℃ (*VIII*).

	Ageing Pressure (MPa)	Initial strength (MPa) [psi]	1-month (MPa) [psi]	3-months (MPa) [psi]	6-months (MPa) [psi]	12-months (MPa) [psi]
Crude oil	50	3.2±0.5 [464±72]	4.4±0.5 [640±72]	4.4±0.7 [640±100]	4.6±0.3 [670±40]	4.4±0.5 [640±72]
Brine	50	3.2±0.5 [464±72]	2.9±0.4 [420±58]	2.5±1.0 [360±145]	2.6±0.3 [380±40]	4.9±0.4 [710±58]
H_2S	1	3.2±0.5 [464±72]	3.2±2.0 [464±290]	3.1±1.0 [450±145]	3.8±0.4 [550±58]	1.2±1.5 [174±218]

Average values and standard deviation from three specimens.

The weight changes of the specimens were measured at different time intervals. All the specimens experienced weight reduction. However, the weight reduction of the specimens exposed to brine was compensated (*VIII*). This could be the effect of alkali leaching (weight reduction) and saturation progress (weight increase). The latter has been studied by Nasvi *et al.* (*2014b*). The weight reduction of the specimens that were exposed to H_2S was substantial due to significant deterioration of the specimens. No relevant study could be found considering the weight changes of geopolymers during a long-term integrity study. Lecolier's work on Portland cement was selected for comparison. Lecolier *et al.* (*2010*) exposed oil well cement specimens to H_2S, crude oil, and brine, for 3, 6, and 12 months, to study their weight changes. Based on their results, Portland cement experienced 1% of weight variation.

Permeability of the geopolymers were only measured before and after a 12-month exposure, **Table 4.6**. The initial permeability was measured to be 0.033

micro-Darcy. The permeability of the specimens, which were exposed to crude oil and brine slightly increased. As the specimens that were exposed to H_2S for 12 months deteriorated, their permeability could not be measured. The measured permeability of Portland cement exposed to H_2S for 12 months, and cured at 120℃, and 0.7 MPa has been reported to be 20 micro-Darcy (*Lecolier et al. 2010*).

Table 4.6 Permeability of the geopolymers aged at 100℃ (*VIII*).

	Ageing Pressure (MPa)	**Initial Permeability (micro-Darcy)**	**12-months Permeability (micro-Darcy)**
Crude oil	50	0.033	0.068
Brine	50	0.033	0.037
H_2S	1	0.033	N/A*

* Not possible to measure due to deterioration of the specimens.

Chapter 5

Conclusion

Geopolymers have been suggested as an alternative to Portland cement, and it is of importance to investigate their applicability as an alternative material for permanent P&A. Therefore, the present study investigated some of the fundamental properties and functional requirement of geopolymers. Based on the obtained results from this study the following conclusions can be drawn:

The particle size of the source material significantly affects the reactivity and properties of the geopolymers.

Sodium-containing geopolymeric systems show a markedly higher viscosity than potassium-containing systems. Albeit, a non-Newtonian behavior was observed for both systems.

The pumpability of geopolymers could effectively be adjusted by the addition of retarders, such as sucrose, to certain dosages (up to 2% of total solid phase) without compromising the mechanical properties of the geopolymers.

Swift exposure of cured geopolymers to air causes cracks, which reduces the mechanical properties. One reason for the breakdown could be the evaporation of water, which is physically bonded or chemically bonded.

A lower concentration of alkali solution can result in a higher strength for geopolymer than a higher concentration of alkali solution when combinations of sodium- and potassium- containing systems are used as activators.

A higher curing temperature of the mixes with higher concentration of alkali solution may activate a consecutive reaction, which could reduce the strength of geopolymers.

The X-ray patterns of the norite-based geopolymers indicated amorphous phases for the sodium-containing systems at 87℃ of curing, while crystallization was expected at elevated temperatures.

The X-ray patterns indicated the formation of the zeolite phase for potassium-containing systems.

Long-term durability experiments show a further reaction after six months of curing takes place and increases the compressive strength and tensile strength of the aplite-based geopolymers that were exposed to crude oil and brine.

The long-term exposure of geopolymers to H_2S deteriorates both the compressive strength and tensile strength of the geopolymers. After six months of curing, as a result of the consecutive reaction, phase(s) is formed which increases the compressive and tensile strengths while interacting with H_2S.

Low permeability, favorable compressive strength, high pH value, and low shrinkage factor of geopolymers are key factors that could indicate a bright future for the geopolymer technology.

Concluding Remark

Geopolymers represent a good alternative to well cements for P&A operations. However, more studies need to be performed to be able to control the geopolymer performance in practical operations. It would also be interesting to study the optimization of setting time and pumpability time of geopolymers.

References

Aadnoy, B., and Looyeh, R. 2011. *Petroleum rock mechanics; Drilling operations and well design*. First edition. Published by: Gulf Professional Publishing Publ. Amsterdam. ISBN: 9780123855466

Abshire, L.W., Desai, P., Mueller, D., et al. 2012. *Offshore permanent well abandonment*. Oilfield Review Spring 2012: 24, no. 1. https://www.slb.com/~/media/Files/resources/oilfield_review/ors12/spr12/or2012spr04_abandon.pdf

Andrade, J. D. 2015. *Cement sheath integrity during thermal cycling*. Doctoral Thesis. Norwegian University of Science and Technology, Trondheim, Norway.

API 10B-2. 2005. *Recommended practice for testing well cements*. First edition. Published by American Petroleum Institute, Washington, USA.

Barclay, I., Pellenbarg, J., Tettero, F., et al. 2001. *The beginning of the end: A review of abandonment and decommissioning practices*. Oilfield Review January 2001: 13, no. 4. http://www.slb.com/~/media/Files/resources/oilfield_review/ors01/win01/p28_41.ashx

Chartier, M.A., Thomson, S., Bordieanu, M., et al. 2008. *Performance of characterization and optimization of cement systems for thermally stimulated wells*. Paper SPE-174493 presented at the SPE Canada Heavy Oil technical Conference held in Calgary, Alberta, Canada, 9-11 June. http://dx.doi.org/10.2118/174493-MS

Cheng, H., Lin, K.L., Cui, R., et al. 2015. *The effect of SiO_2/Na_2O molar ratio on the characteristics of alkali-activated waste catalyst-metakaolin based geopolymers*. Journal of Construction and Building Materials 95 (2015) 710-720. http://dx.doi.org/10.1016/j.conbuildmat.2015.07.028

Criado, M., Palomo, A., and Jimenez, A.F. 2009. *Alkali activated fly ash: effect of admixtures on paste rheology*. Journal of Rheologica Acta (2009) 48:447-455. http://dx.doi.org/10.1007/s00397-008-0345-5

Davidovits, J. 2005. *Geopolymer, green chemistry and sustainable development solutions*. Published by Geopolymer Institute, Saint-Quentin, France. ISBN 2-9514820-0-0.

Davidovits, J. 2011. *Geopolymer Chemistry & Applications*. Third edition. Saint-Quentin: Institut Geopolymere. ISBN 9782951482050.

Deb, P.S., Nath, P., and Sarker, P.K. 2015. *Drying shrinkage of slag blended fly ash geopolymer concrete cured at room temperature*. Journal of Proceedia Engineering 125 (2015) 594-600. http://dx.doi.org/10.1016/j.proeng.2015.11.066

Deventer, van J.S.J., Provis, J.L., Duxson, P. and Lukey, G.C. 2007. *Reaction mechanisms in the geopolymeric convention of inorganic waste to useful products*. Journal of Hazardous Materials A139 (2007) 506-513. http://dx.doi.org/10.1016/j.jhazmat.2006.02.044

References

EN 450-1:2012. *Fly ash for concrete. Definition, specifications and conformity criteria*. Publication date August 2012. ISBN 978 0 580 70538 0.

Fernandez, A., and Palomo A. 2003. *Characterisation of fly ashes. Potential reactivity as alkaline cements*. Journal of Fuel 82 (2003) 2259-2265. http://dx.doi.org/10.1016/S0016-2361(03)00194-7

Ferone, C., Liguori, B., Capasso, I., et al. 2015. *Thermally treated clay sediments as geopolymer source material*. Journal of Applied Clay Science 107 (2015) 195-204. http://dx.doi.org/10.1016/j.clay.2015.01.027

Fjær, E. 2008. *Petroleum related rock mechanics*. Second edition. Published by Elsevier, Amsterdam, Netherlands. ISBN 9780080557090.

Fjær, E., Holt, R.M., Horsrud, P., et al. 2008. *Petroleum related rock mechanics*. Second edition. Published by: Elsevier, Amsterdam, Netherlands. ISBN 978-0-444-50260-5.

Fronks, R.C. 2002. *International Regulations – Meeting the challenges*. Paper SPE 73879 presented at the SPE International Conference on Health, Safety and Environment in Oil & Gas Exploration and Production held in Kuala Lumpor, Malaysia, 20-22 March. http://dx.doi.org/10.2118/73879-MS

Garcia-Lodeiro, I., Palomo, A., Frnandez-Jimenez, A., and Macphee, D.E. 2011. *Compatibility studies between N-A-S-H and C-A-S-H gels. Study in the ternary diagram Na_2O-CaO-Al_2O_3-SiO_2-H_2O*. Journal of Cement and Concrete Research 41 (2011) 923-931. http://dx.doi.org/10.1016/j.cemconres.2011.05.006

Gherardi, F., Audigane, P., and Gaucher, E.C. 2012. *Predicting long-term geochemical alteration of wellbore cement in a generic geological CO_2 confinement site: Tackling a difficult reactive transport modeling challenge*. Journal of Hydrology 420-421 (2012) 340-359. http://dx.doi.org/10.1016/j.jhydrol.2011.12.026

Hammersley P., Svensson S.O., Hanfland M., et al. 1996. *Two-Dimensional detector software: from real detector to idealized image or two-theta scan*. High Pressure Research, 14 (1996) 235-248.

He, J., Jie, Y., Zhang, J., et al. 2013. *Synthesis and characterization of red mud and rice husk ash-based geopolymer composites*. Journal of Cement and Concrete Composites 37 (2013) 108-118. http://dx.doi.org/10.1016/j.cemconcomp.2012.11.010

Hounsi, A.D., Lecomte-Nana, G., Djeteli, G., et al. 2014. *How does Na, K alkali metal concentration change the early age structural characteristic of kaolin-based geopolymers*. Journal of Ceramics International 40 (2014) 8953-8962. http://dx.doi.org/10.1016/j.ceramint.2014.02.052

Hwang, C.L., and Huynh, T.P. 2015. *Effect of alkali activator and rice husk ash content on the strength development of fly ash and residual rice husk ash-based geopolymers*. Journal of Construction and Building Materials 101 (2015) 1-9. http://dx.doi.org/10.1016/j.conbuildmat.2015.10.025

References

Jang, J.G., and Lee, H.K. 2016. *Effect of fly ash characteristics on delayed high-strength development of geopolymers*. Journal of Construction and Building Materials 102 (2016) 260-269. http://dx.doi.org/10.1016/j.conbuildmat.2015.10.172

Kong, D.L.Y., and Sanjayan, J.G. 2010. *Effect of elevated temperatures on geopolymer paste, mortar and concrete*. Journal of Cement and Concrete Research 40 (2010) 334-339. http://dx.doi.org/10.1016/j.cemconres.2009.10.017

Lecolier, E., Rivereau, A., Ferrer, N. et al. 2010. *Durability of oilwell cement formulations aged in H_2S-containing fluids*. Journal of SPE Drilling & Completion. March 2010. http://dx.doi.org/10.2118/99105-PA

Liversidge, D., Taoutaou, S., Agarwal, S. 2006. *Permanent plug and abandonment solutions for the North Sea*. Paper SPE 100771 presented at the SPE Asia Pacific Oil & Gas Conference and Exhibition held in Adelaide, Australia, 11-13 September. http://dx.doi.org/10.2118/100771-MS

Nasvi, M.C.M., Ranjith, P.G., and Sanjayan, J. 2015. *A Numerical study of triaxial mechanical behaviour of geopolymer at different curing temperatures: An application for geological sequestration wells*. Journal of Natural Gas Science and Engineering 26 (2015) 1148-1160. http://dx.doi.org/10.1016/j.jngse.2015.08.011

Nasvi, M.C.M., Ranjith, P.G., Sanjayan, J., and Bui, H. 2014a. *Effect of temperature on permeability of geopolymer: A primary well sealant for carbon capture and storage wells*. Journal of Fuel 117 (2014) 354-363. http://dx.doi.org/10.1016/j.fuel.2013.09.007

Nasvi, M.C.M., Ranjith, P.G., Sanjayan, J., et al. 2014b. *Mechanical behaviour of wellbore materials saturated in brine water with different salinity levels*. Journal of Energy 66 (2014) 239-249. http://dx.doi.org/10.1016/j.energy.2013.12.003

Nath, P., and Sarker, P.K. 2014. *Effect of GGBFS on setting, workability and early strength properties of fly ash geopolymer concrete cured in ambient condition*. Journal of Construction and Building Materials 66 (2014) 163-171. http://dx.doi.org/10.1016/j.conbuildmat.2014.05.080

Nelson, E.B., and Guillot, D. 2006. *Well Cementing*. Second edition. Texas: Schlumberger. ISBN-10: 0 9788530 0 8

Nesse W.D. 2000. *Introduction to mineralogy*. New York (NY): Oxford University. Press; 2000. Printed in United States of America. ISBN: 0-19-510691-1.

Nikolic, V., Komljenovic, M., Bascarevic, Z., et al. 2015. *The influence of fly ash characteristics and reaction conditions on strength and structure of geopolymers*. Journal of Construction and Building Materials 94 (2015) 361-370. http://dx.doi.org/10.1016/j.conbuildmat.2015.07.014

NORSOK D-010. 2013. *Well Integrity in Drilling and Well Operations*. Fourth Edition. Lysaker: Standard Norway.

References

Norwegian Petroleum Directorate. 2015. http://factpages.npd.no/factpages/Default.aspx?culture=en&nav1=wellbore&nav2=Statistics%7cEntryYear (accessed 20 June 2015)

Oil & Gas UK. 2012a. *Guidelines for Suspension and Abandonment of Wells*. Issue 4. London: The United Kingdom Offshore Oil and Gas Industry Association Limited. ISBN: 1 903 003 84 2.

Oil & Gas UK. 2012b. *Guidelines for Qualification of Materials for the Suspension and Abandonment of Wells*, issue 1. London: The United Kingdom Offshore Oil and Gas Industry Association Limited. ISBN: 1 903 003 85 4.

Ozer, I., and Soyer-Uzun, S. 2015. *Relations between the structural characteristics and compressive strength in metakaolin based geopolymers with different molar Si/Al ratios*. Journal of Ceramics International 41 (2015) 10192-10198. http://dx.doi.org/10.1016/j.ceramint.2015.04.125

Pacheco-Torgal, F., Labrincha, J.A., Leonelli, C., et al. 2015. *Handbook of alkali-activated Cements, Mortars and Concretes*. First edition. Woodhead Publishing Limited. ISBN 978-1-78242-288-4.

Provis, J.L. and van Deventer, J.S.J. 2009. *Geopolymers Structure, processing, properties and industrial applications*. First edition. Published by: Woodhead Publishing Limited. ISBN 978-1-84569-638-2.

Puertas, F., Varga, C., and Alonso, M.M. 2014. *Rheology of alkali-activated slag pastes. Effect of the nature and concentration of the activating solution*. Journal of Cement & Concrete Composites 53 (2014) 279-288. http://dx.doi.org/10.1016/j.cemconcomp.2014.07.012

Rattansak, U., Pankhet, K., and Chindaprasirt, P. 2011. *Effect of chemical admixtures on properties of high-calcium fly ash geopolymers*. International Journal of Minerals, Metallurgy and Materials: Volume 18, Number 3, June 2011, Page 364. http://dx.doi.org/10.1007/s12613-011-0448-3

Ravikumar, D., Peethamparan, S., and Neithalath, N. 2010. *Structure and strength of NaOH activated concretes containing fly ash or GGBFS as the sole binder*. Journal of Cement & Concrete Composite 32 (2010) 399-410. http://dx.doi.org/10.1016/j.cemconcomp.2010.03.007

Reddy, B.R., Santra, A., McMechan, D., et al. 2005. *Cement mechanical property measurements under wellbore conditions*. Paper SPE-95921 presented at the 2005 SPE Annual Technical Conference and Exhibition held in Dallas, Texas, USA., 9-12 October 2005. http://dx.doi.org/10.2118/95921-MS

Reddy, B.R., Xu, Y., Ravi, K., et al. 2009. *Cement-shrinkage measurement in oilwell cementing-A comparative study of laboratory methods and procedures*. SPE drilling & Completion March 2009 Volume 24, issue 01. http://dx.doi.org/10.2118/103610-PA

References

Romagnoli, M., Leonelli, C., Kasme, E., and Gualtieri, M.L. 2012. *Rheology of geopolymer by DOE approach*. Journal of Construction and Building Materials 36 (2012) 251-258. http://dx.doi.org/10.1016/j.conbuildmat.2012.04.122

Ryu, G.S., lee, Y.B., Koh, K.T., and Chung, Y.S. 2013. *The mechanical properties of fly ash-based geopolymer concrete with alkaline activators*. Journal of Construction and Building Materials 47 (2013) 409-418. http://dx.doi.org/10.1016/j.conbuildmat.2013.05.069

Salih, M.A., Farzadina, N., Abang Ali, A.A., and Demirboga, R. 2015. *Effect of different curing temperatures on alkali activated palm oil fuel ash paste*. Journal of Construction and Building Materials 94 (2015) 116-125. http://dx.doi.org/10.1016/j.conbuildmat.2015.06.052

Satoh, H., Shimoda, S., Yamaguchi, K., et al. 2013. *The long-term corrosion behavior of abandoned wells under CO_2 geological storage conditions: (1) Experimental results for cement alteration*. Journal of Energy Procedia 37 (5781-5792. http://dx.doi.org/10.1016/j.egypro.2013.06.501

Singh, B., Ishwarya, G., Gupta, M., and Bhattacharyya, S.K. 2015. *Geopolymer concrete: A review of some recent developments*. Journal of Construction and Building Materials 85 (2015) 78-90. http://dx.doi.org/10.1016/j.conbuildmat.2015.03.036

Waseda, Y., Matsubara, E., Shinoda, K. 2011. *X-ray diffraction crystallography*. First edition. Published by: Springer-Verlag Berlin. ISBN 978-3-642-16635-8.

Yusuf, M.O., Johari, M.A.M., Ahmad, Z.A., and Maslehuddin, M. 2014. *Influence of curing methods and concentration of NaOH on strength of the synthesized alkaline activated ground slag-ultra-fine palm oil fuel ash mortar/concrete*. Journal of Construction and Building Materials 66 (2014) 541-548. http://dx.doi.org/10.1016/j.conbuildmat.2014.05.037

Zhang, M., El-Korchi, T., Zhang, G., et al. 2014. *Synthesis factors affecting mechanical properties, microstructure, and chemical composition of red mud-fly ash based geopolymers*. Journal of Fuel 134 (2014) 315-325. http://dx.doi.org/10.1016/j.fuel.2014.05.058